

A theory vade mecum for PSI experiments

G. Colangelo¹, F. Hagelstein², A. Signer^{2*}, and P. Stoffer³

1 Albert Einstein Center for Fundamental Physics, Institute for Theoretical Physics,
University of Bern, Switzerland

2 Paul Scherrer Institut, 5232 Villigen PSI, Switzerland

3 University of Vienna, Faculty of Physics, Boltzmannngasse 5, 1090 Vienna, Austria

* adrian.signer@psi.ch

July 14, 2021



Review of Particle Physics at PSI
doi:[10.21468/SciPostPhysProc.2](https://doi.org/10.21468/SciPostPhysProc.2)

Abstract

This article gives a compact introduction and overview of the theory underlying the experiments described in the rest of this review.

5.1 Introduction

The purpose of this article is to give a broad overview of the theory background to the experiments that have been and are carried out at the Paul Scherrer Institute. Space limitations make it impossible to go into depth or provide a self-contained theoretical summary. Much more modestly, we aim to put the experiments into context and provide key references for further reading. The experiments we refer to are listed in Table 5.1 and they will be described in greater detail in separate sections/articles of the Review of Particle Physics at PSI [1–23]. These experiments either lead to precise determinations of physical parameters required as input for other experiments (e.g., muon life time, pion mass), or search for physics beyond the Standard Model (BSM). The BSM searches proceed along different frontiers. One way to search for new physics is to consider physical observables whose Standard Model (SM) contributions either vanish or are too small to be experimentally accessible. In other words, they are identical to zero for practical purposes. Examples are charged lepton-flavor violating (cLFV) muon decays or a permanent neutron electric dipole moment (EDM). To put constraints on the branching ratios of BSM decays, one has to observe a large number of decays. This is, thus, called a search at the intensity frontier. Another way to search for new physics is to consider precision observables and search for deviations from the SM expectations. Prominent examples are the precision QED tests with muonium, as well as the precision laser spectroscopy experiments with muonic atoms. These are, thus, called searches at the precision frontier. The low-energy experiments at PSI are complementary to the experiments at LHC, which sit at the energy frontier.

After a general overview of the theoretical methods applied to describe the processes and bound states in Table 5.1, we will, in turn, consider the muon, the proton, nucleons and nuclei, the free neutron, and the pions.

5.2 Overview

The experiments we are primarily concerned with involve low-energy interactions of electrons, muons, protons, neutrons, and pions. In Section 5.2.1 we first describe these interactions in

experiment	section	process / particles / (bound states)
[1] muon decay	6	$\mu^+ \rightarrow e^+ \nu_e \bar{\nu}_\mu$
[2] MuLan	16	$\mu^+ \rightarrow e^+ \nu_e \bar{\nu}_\mu$
[3] SINDRUM	7	$\mu^+ \rightarrow e^+ ee, \mu^+ \rightarrow e^+ \nu_e \bar{\nu}_\mu ee, \pi^+ \rightarrow e^+ \nu_e ee, \pi^0 \rightarrow ee$
[4] SINDRUM II	8	$\mu^- \frac{A}{Z}N \rightarrow e^- \frac{A}{Z}N$ for Au, Pb, Ti
[5] MEG	19	$\mu^+ \rightarrow e^+ \gamma, \mu^+ \rightarrow e^+ \nu_e \bar{\nu}_\mu \gamma, \mu^+ \rightarrow e^+ X \rightarrow e^+ \gamma \gamma$
[6] Mu3e	20	$\mu^+ \rightarrow e^+ ee, \mu^+ \rightarrow e^+ \nu_e \bar{\nu}_\mu ee$
[7] Mspec, Mu-Mass	29	$M = (\mu^+ e^-), \mu^+$
[8] MACS	9	$M = (\mu^+ e^-) \leftrightarrow \bar{M} = (\mu^- e^+)$
[9] CREMA	21	$(\mu^- p), (\mu^- d), (\mu^- \text{He}), p, d, \text{He}$
[10] muX	22	$(\mu^- \frac{A}{Z}N), {}^{248}_{96}\text{Cm}, {}^{226}_{88}\text{Ra}$
[11] MUSE	23	$e^\pm p \rightarrow e^\pm p, \mu^\pm p \rightarrow \mu^\pm p$
[12] MuCap	17	$\mu^- p \rightarrow \nu_\mu n$
[13] MuSun	18	$\mu^- d \rightarrow \nu_\mu nn$
[14] pionic deuterium	14	$(\pi^- p), (\pi^- d)$
[15] pionic helium	26	$(\pi^- e^- {}^4\text{He}^{++}), \pi^-$
[16] nTRV	15	$n \rightarrow pe^- \bar{\nu}_e$
[17] nEDM	27	n, n
[18] nEDMX	28	n / dark matter / exotic
[19] negative pions	10	$(\pi^- p), \pi^-$
[20] positive pions	11	$\pi^+ \rightarrow \mu^+ \nu_\mu, \pi^+, \nu_\mu$
[21] neutral pions	12	$\pi^- p \rightarrow \pi^0 n, \pi^0$
[22] PiBeta	24	$\pi^+ \rightarrow \pi^0 e^+ \nu_e, \pi^+ \rightarrow e^+ \nu_e (+\gamma), \mu^+ \rightarrow e^+ \nu_e \bar{\nu}_\mu \gamma$
[23] PEN	25	$\pi^+ \rightarrow e^+ \nu_e (+\gamma), \mu^+ \rightarrow e^+ \nu_e \bar{\nu}_\mu \gamma$

Table 5.1: Processes and particles (bound states) that are investigated at PSI, where the driving interaction to be studied is indicated by the color as follows: **BSM**, **weak**, **weak and try to learn about strong**, **EM**, **EM and try to learn about strong**, **strong**. In addition the mass or charge radius of particles are measured. The section number refers to the Review of Particle Physics at PSI.

40 the SM before we discuss the generalisation to BSM scenarios in Section 5.2.2. While the
 41 theoretical methods for these cases are dominated by perturbative expansions in the couplings,
 42 Section 5.2.3 is devoted to hadronic effects that often play an important part in low-energy
 43 experiments.

44 5.2.1 Standard Model at low energies

45 In the SM the dynamics of the particles listed above is described by the gauge theory of strong
 46 and electroweak interactions. In view of the large masses of the Higgs and weak gauge bosons,
 47 the weak part of the SM Lagrangian is essentially frozen at low energies (it will later be con-
 48 sidered as a small correction). In this regime, the SM reduces to the standard QED and QCD
 49 Lagrangian

$$\mathcal{L}_{\text{QED+QCD}} = \sum_f \bar{f} (i\not{D} - m_f) f - \frac{1}{4} F_{\alpha\beta} F^{\alpha\beta} - \frac{1}{4} G_{\alpha\beta} G^{\alpha\beta}, \quad (5.1)$$

50 where the electromagnetic and gluonic field-strength tensors are expressed in terms of the
 51 photon and gluon fields, A^α and G^α , as $F^{\alpha\beta} = \partial^\alpha A^\beta - \partial^\beta A^\alpha$, $G^{\alpha\beta} = \partial^\alpha G^\beta - \partial^\beta G^\alpha - ig_s [G^\alpha, G^\beta]$,
 52 and where for clarity we have omitted gauge-fixing and ghost terms. The sum runs over all
 53 fermions of mass m_f , electric charge eQ_f , and color charge $g_s t_f^a$, and the covariant derivative
 54 acts on the fermion fields as $D_\alpha f = (\partial_\alpha - ieQ_f A_\alpha - ig_s t_f^a G_\alpha^a) f$. For $f = \ell \in \{e, \mu, \tau\}$ we have
 55 $Q_\ell = -1$ and $t_\ell^a = 0$, whereas for quarks $Q_u = 2/3$, $Q_d = -1/3$, and $t_{u,d}^a = \lambda^a/2$ with Gell-
 56 Mann matrices λ^a . In several experiments of interest here the photon acts as a probe: it is
 57 coupled to the electromagnetic current J_{em}^α as

$$\mathcal{L}_{\text{QED}}^{\text{int}} = e A_\alpha J_{\text{em}}^\alpha \equiv e A_\alpha \sum_f Q_f \bar{f} \gamma^\alpha f. \quad (5.2)$$

58 If we use (5.1) to compute the matrix element of J_{em}^α between two states of pointlike leptons
 59 ℓ with momenta p_1 and $p_2 = p_1 + q$, we find

$$\langle \ell(p_2) | J_{\text{em}}^\alpha | \ell(p_1) \rangle = \bar{u}(p_2, m_\ell) \left(F_1^{(\ell)}(q^2) \gamma^\alpha + F_2^{(\ell)}(q^2) \frac{i \sigma^{\alpha\beta} q_\beta}{2m_\ell} \right) u(p_1, m_\ell), \quad (5.3)$$

60 where u and \bar{u} are the usual spinors. The decomposition (5.3) directly follows from the Lorentz
 61 and $U(1)_{\text{em}}$ gauge symmetries of the theory and is valid beyond perturbation theory. While
 62 $F_1^{(\ell)}$ is related to the electric charge, $F_2^{(\ell)}$ is related to the anomalous magnetic moment (AMM)
 63 of ℓ as

$$F_2^{(\ell)}(0) = a_\ell = \frac{(g-2)_\ell}{2}. \quad (5.4)$$

64 In contrast to the leptons, quarks do not appear as free particles in nature, but are confined
 65 inside hadrons by the strong interaction. The general principles on which the decomposi-
 66 tion (5.3) is based, also hold for non-pointlike particles, such as the nucleons $N \in \{p, n\}$

$$\langle N(p_2) | J_{\text{em}}^\alpha | N(p_1) \rangle = \bar{u}(p_2, m_N) \left(F_1^{(N)}(Q^2) \gamma^\alpha + F_2^{(N)}(Q^2) \frac{i \sigma^{\alpha\beta} q_\beta}{2m_N} \right) u(p_1, m_N), \quad (5.5)$$

67 where we have introduced the common definition $Q^2 \equiv -q^2$. A relation between the AMM
 68 and $F_2^{(N)}$ analogous to (5.4) still holds. However, this quantity depends on strong dynamics,
 69 which at low energies cannot be computed in perturbation theory.

70 In the case of the nucleons, often the electric and magnetic form factors

$$G_E^{(N)}(Q^2) \equiv F_1^{(N)}(Q^2) - \frac{Q^2}{4m_N^2} F_2^{(N)}(Q^2), \quad G_M^{(N)}(Q^2) \equiv F_1^{(N)}(Q^2) + F_2^{(N)}(Q^2) \quad (5.6)$$

71 are used. In the limit of small Q^2 all form factors $F_i(Q^2)$ can be understood as the Fourier trans-
72 form of an extended classical ‘charge’ distribution $\rho_i(r)$ in the Breit frame where $q^\mu = (0, \vec{q})$.
73 Upon expansion in small Q^2 we get

$$F_i(Q^2) = \int d^3\vec{r} e^{-i\vec{q}\cdot\vec{r}} \rho_i(r) = \int d^3\vec{r} \rho_i(r) - \frac{1}{6} Q^2 \int d^3\vec{r} r^2 \rho_i(r) + \dots \quad (5.7)$$

74 This leads to a general expression for the second moment of the charge distribution ρ_i

$$r_i^2 \equiv \frac{1}{N} \int d^3\vec{r} r^2 \rho_i(r) = -6 \frac{1}{N} \left. \frac{dF_i(Q^2)}{dQ^2} \right|_{Q^2=0}, \quad N = \begin{cases} 1 & \text{if } F_i(0) = 0, \\ F_i(0) & \text{else.} \end{cases} \quad (5.8)$$

75 The relation above is used for example to determine the root-mean-square, $R_i = \sqrt{r_i^2}$, charge
76 and magnetic radii of the proton as well as the axial radius of the nucleon.

77 If we now consider the weak interactions, we must arrange fermions into left-handed dou-
78 blets and right-handed singlets. An important role for low-energy processes is played by the
79 charged weak current

$$J_{cc}^\alpha = \sum_\ell \bar{\nu}_\ell \gamma^\alpha P_L \ell + \sum_{ij} V_{ij} \bar{u}_i \gamma^\alpha P_L d_j, \quad (5.9)$$

80 which couples only to left-handed fermions, $P_L \equiv (1 - \gamma_5)/2$. In the sum over the quark-
81 field terms, the CKM matrix V_{ij} describes the flavor-changing effects of the weak interactions.
82 Including for completeness also the neutral weak current J_{nc}^α , the interactions of (5.2) are
83 modified to

$$\mathcal{L}_{EW}^{\text{int}} = e A_\alpha J_{em}^\alpha + \frac{g}{\sqrt{2}} (W_\alpha^+ J_{cc}^\alpha + \text{h.c.}) + g_Z Z_\alpha J_{nc}^\alpha, \quad (5.10)$$

84 where $g = e/\sin \theta_W$, $g_Z = g/\cos \theta_W$ are the weak $SU(2)_L$ couplings that can be expressed in
85 terms of e and the electroweak mixing (Weinberg) angle θ_W . At the typical energy of processes
86 considered here, much smaller than m_W and m_Z , the W and Z boson masses, we can integrate
87 out the W and Z bosons and adopt an effective field theory (EFT) approach. This results in
88 the Fermi theory of current-current interactions

$$\mathcal{L}_{4F} = -\frac{4G_F}{\sqrt{2}} (J_{cc}^\alpha (J_{cc})_\alpha^\dagger + J_{nc}^\alpha (J_{nc})_\alpha), \quad (5.11)$$

89 where $4G_F/\sqrt{2} = g^2/(2m_W^2)$ is the matching (Wilson) coefficient at tree level. Using (5.9)
90 (and the corresponding expression for J_{nc}^α) to express \mathcal{L}_{4F} in terms of fermion fields we end
91 up with vector contact interactions. They correspond to dimension-6 four-fermion vector op-
92 erators of the generic form

$$[O_{\{\ell/q\}}^{V,XY}]_{ijkl} = (\bar{\psi}_i \gamma^\alpha P_X \psi_j) (\bar{\psi}_k \gamma_\alpha P_Y \psi_l), \quad (5.12)$$

93 where $X, Y \in \{L, R\}$ and $\{i, j, k, l\}$ are generation indices. The notion ‘vector’ refers to the
94 Lorentz structure of the bilinears, which in turn is closely related to the nature of the exchange
95 particle that is integrated out. Since the fermion fields ψ_i can be quarks or leptons of any
96 generation, there are in principle quite a lot of different operators. However, only a subset of

97 those are generated by integrating out the W and Z fields. In particular, there are no charged
 98 cLFV operators due to an accidental symmetry of the SM.

99 Because the masses of the top quark and the Higgs boson are of the same order as m_W ,
 100 these fields can also be integrated out. Operators beyond the four-fermion vector operators
 101 appear in the SM with an additional suppression, such as scalar dimension-6 four-fermion
 102 operators

$$[O_{\{\ell/q\}}^{S,XY}]_{ijkl} = (\bar{\psi}_i P_X \psi_j) (\bar{\psi}_k P_Y \psi_l), \quad X, Y \in \{L, R\}, \quad (5.13)$$

103 which are parametrically suppressed by Yukawa couplings [24], or dimension-5 dipole opera-
 104 tors (and their Hermitian conjugate)

$$[O_{\{\ell/q\}\gamma}^D]_{ij} = (\bar{\psi}_i \sigma_{\alpha\beta} P_R \psi_j) F^{\alpha\beta}, \quad [O_{qG}^D]_{ij} = (\bar{\psi}_i \sigma_{\alpha\beta} G^{\alpha\beta} P_R \psi_j), \quad (5.14)$$

105 which appear at the loop level. Thus, we arrive at an EFT that consistently describes low-
 106 energy processes. It only contains fields with masses much lower than m_W . In particular, the
 107 photon and the gluons are the only gauge bosons present. The gauge symmetry of the SM,
 108 $SU(3)_c \times SU(2)_L \times U(1)_Y$, is reduced to the gauge symmetry of QCD and QED, $SU(3)_c \times U(1)_{\text{em}}$.
 109 The effect of the heavy degrees of freedom of the SM is encoded in the Wilson coefficients that
 110 multiply the operators, with G_F in (5.11) being one such example.

111 5.2.2 Low-energy physics beyond the Standard Model

112 Many of the experiments listed in Table 5.1 are motivated by the search for new physics. One
 113 can think of a plethora of BSM scenarios. They rely on different interaction mechanisms, and
 114 can be roughly classified based on the masses of the BSM particles and their coupling strengths.

115 Light BSM particles should only have a small coupling to SM particles, which would ex-
 116 plain their small contribution to physical observables. The most prominent examples are dark
 117 photons, axions, or axion-like particles (ALPs). The axion has been proposed as a dynami-
 118 cal solution to the strong CP problem [25–28], i.e., the ‘‘naturalness’’ problem of the small
 119 QCD θ parameter. It is introduced as the Nambu-Goldstone boson associated with a sponta-
 120 neously broken additional global $U(1)_{\text{PQ}}$ symmetry of the SM Lagrangian. The modified SM
 121 Lagrangian reads

$$\begin{aligned} \mathcal{L}_{\text{SM}}^{\text{eff}} &= \mathcal{L}_{\text{SM}} + \mathcal{L}_{\text{int}}[\partial^\mu a_{\text{phys.}}/f_a; \psi] \\ &\quad - \frac{1}{2} \partial^\mu a_{\text{phys.}} \partial_\mu a_{\text{phys.}} - \frac{m_a^2}{2} a_{\text{phys.}}^2 + \frac{a_{\text{phys.}}}{f_a} \zeta \frac{g_s^2}{32\pi^2} \tilde{G}_{\alpha\beta} G^{\alpha\beta}, \end{aligned} \quad (5.15)$$

122 where $a_{\text{phys.}} = a - \langle a \rangle$ is the physical axion field with mass m_a , and f_a is the $U(1)_{\text{PQ}}$ symme-
 123 try breaking scale. The axion is a pseudoscalar that couples derivatively to any field ψ . In
 124 addition, because of the chiral anomaly of the $U(1)_{\text{PQ}}$ current, it directly couples to the gluon
 125 density, where ζ is a model-dependent parameter. The minimum of the effective potential
 126 occurs at the axion vacuum expectation value $\langle a \rangle = -\theta f_a / \zeta$, which leads to a cancellation
 127 of the CP violating QCD θ term and dynamically solves the strong CP problem. The defining
 128 characteristic of the axion, distinguishing it from an ALP, is $m_a f_a \sim m_\pi f_\pi$. This follows from
 129 mixing of the axion with the light π and η mesons.

130 In the following, we will be mainly concerned with heavy BSM particles. In Section 5.2.1,
 131 we described how the W and Z bosons can be integrated out in an EFT approach. Similarly,
 132 whatever BSM physics there is, as long as it respects QED and QCD gauge symmetry and in-
 133 volves degrees of freedom with a ‘large’ mass scale Λ , it can be integrated out and its effects will
 134 be encoded in Wilson coefficients of gauge-invariant higher-dimensional operators. Operators
 135 that were absent in the SM case might now be generated. Thus, we are led to write down the

136 most general relativistic Lagrangian that respects electromagnetic $U(1)_{\text{em}}$ and strong $SU(3)_c$
 137 gauge invariance and obtain a general low-energy effective field theory (LEFT)

$$\mathcal{L}_{\text{LEFT}} = \mathcal{L}_{\text{QED+QCD}} + \frac{1}{\Lambda} \sum_i C_i^{(5)} O_i^{(5)} + \frac{1}{\Lambda^2} \sum_j C_j^{(6)} O_j^{(6)} + \dots \quad (5.16)$$

138 Here Λ is the scale of physics that is not dynamically described by the degrees of freedom
 139 present in $\mathcal{L}_{\text{LEFT}}$. If we include all charged leptons and all quarks apart from the top in $\mathcal{L}_{\text{LEFT}}$,
 140 the scale Λ is assumed to be larger than the mass of the b quark but not larger than the
 141 electroweak scale m_W . The sums i and j run over all possible operators of dimension 5 and
 142 6, respectively. Typically, operators of dimension larger than 6 are neglected. $O^{(5)}$ and $O^{(6)}$
 143 denote the operators, $C^{(5)}$ and $C^{(6)}$ are the corresponding Wilson coefficients. Operators that
 144 are related through Fierz identities or those that can be eliminated through equations of motion
 145 are not included. Naturally, the choice of the operator basis is not unique, but a complete basis
 146 up to dimension 6 can be found in [24].

147 The Lagrangian (5.16) provides a consistent quantum-field theoretical framework to relate
 148 low-energy measurements to the determination of parameters of the SM and constraints on
 149 BSM physics. Many different routes have been taken to generically parametrize low-energy
 150 observables and measuring or constraining the associated parameters. The prime example is
 151 the Michel decay, where an analysis with initially a single parameter [29] was generalized and
 152 written in terms of parameters related to scalar, vector and tensor contact interactions¹ [30].
 153 A similar effort has been made for cLFV decays $\mu \rightarrow e\gamma$ and $\mu \rightarrow eee$ considering lepton-flavor-
 154 violating contact interactions [31].

155 At first sight this is very similar to constraining the Wilson coefficients of (5.16). Indeed,
 156 the bulk of the operators of (5.16) are also scalar, vector and tensor interactions. However, the
 157 Wilson coefficients are well-defined couplings of a quantum field theory. In particular, typically
 158 they run and mix under renormalization-group evolution (RGE). If a low-energy observable
 159 is expressed in terms of Wilson coefficients, they are understood to be evaluated at the low
 160 scale, $C_i^{(n)}(m_\mu)$. On the other hand, to relate the Wilson coefficients of the EFT to a BSM
 161 model, the heavy degrees of freedom of the latter have to be integrated out. This yields the
 162 Wilson coefficients at the high scale, $C_i^{(n)}(\Lambda)$. Including RGE of $C_i^{(n)}(\Lambda)$ to $C_i^{(n)}(m_\mu)$ is not in
 163 the first instance about increasing precision, but to include qualitatively new effects through
 164 mixing. This has a profound impact on using low-energy measurements to constrain BSM
 165 models.

166 Of course, it is also possible that BSM physics appears only at a scale much larger than
 167 m_W . If this is the case, in a first step another effective theory has to be used, the SM effective
 168 field theory (SMEFT). This is a theory similar to (5.16), but with all fields and symmetries of
 169 the SM. It contains all operators $\mathcal{O}_i^{(n)}$ expressed in terms of the SM gauge fields, the Higgs
 170 doublet, as well as left-handed doublet and right-handed singlet fermion fields that respect
 171 the SM gauge symmetry $SU(3)_c \times SU(2)_L \times U(1)_Y$,

$$\mathcal{L}_{\text{SMEFT}} = \mathcal{L}_{\text{SM}} + \frac{1}{\Lambda} (C^{(5)} \mathcal{O}^{(5)} + \text{h.c.}) + \frac{1}{\Lambda^2} \sum_j C_j^{(6)} \mathcal{O}_j^{(6)} + \dots \quad (5.17)$$

172 SMEFT has only one dimension-5 operator $\mathcal{O}^{(5)}$ (and its Hermitian conjugate). This is the
 173 Weinberg operator [32] that is associated with neutrino masses. At dimension 6 there are
 174 numerous operators, some of which violate baryon number. As for $\mathcal{L}_{\text{LEFT}}$ different bases are
 175 possible, but the so-called Warsaw basis [33] is used frequently.

176 In the case $\Lambda \gg m_W$ the input of the BSM model is given through Wilson coefficients
 177 $C_i^{(n)}(\Lambda)$. Then, the RGE is used to obtain $C_i^{(n)}(m_W)$. In a next step, SMEFT is matched to

¹ Section 6: Muon decay [1]

178 LEFT at the electroweak scale. This means that $C_i^{(n)}(m_W)$ are expressed in terms of $C_i^{(n)}(m_W)$.
 179 Finally, the Wilson coefficients of LEFT, $C_i^{(n)}(m_W)$, are run with the RGE of LEFT from the scale
 180 m_W to the low scale m_μ , and we are ready to express physical low-energy observables. The
 181 complete dimension-6 RGEs of SMEFT and LEFT, and the matching equations between the two
 182 EFTs are known at one loop [34–38], whereas beyond only partial results are known.

183 Now that we have a framework that incorporates the effects of the full SM and potential
 184 BSM physics on low-energy observables, we can return to our starting point, the matrix ele-
 185 ments of the electromagnetic currents. Moving from (5.1) to (5.16) leads to a generalization
 186 of (5.2), (5.3), and (5.5). In particular, the current itself is modified and includes additional
 187 terms from the dimension-5 dipole operators. The most general expression for a vector current
 188 depending on p_1 and p_2 can be written as combination of six possible structures: γ^α , $\gamma^\alpha\gamma_5$, q^α ,
 189 $q^\alpha\gamma_5$, $q_\beta\sigma^{\alpha\beta}$ and $q_\beta\sigma^{\alpha\beta}\gamma_5$. Replacing $q = p_2 - p_1$ by $p_2 + p_1$ does not lead to new independent
 190 structures, as can be shown by using the Dirac equation. Since the electromagnetic current is
 191 conserved $\partial_\alpha J_{\text{em}}^\alpha = 0$ only four terms remain and we get

$$\begin{aligned} \langle f(p_2) | J_{\text{em}}^\alpha | f(p_1) \rangle = & \bar{u}(p_2, m_f) \left(F_1^{(f)}(q^2) \gamma^\alpha + (F_2^{(f)}(q^2) - i \gamma_5 F_3^{(f)}(q^2)) \frac{i \sigma^{\alpha\beta} q_\beta}{2 m_f} \right. \\ & \left. + F_4^{(f)}(q^2) \frac{1}{m_f^2} (q^2 \gamma^\alpha - 2 m_f q^\alpha) \gamma_5 \right) u(p_1, m_f). \end{aligned} \quad (5.18)$$

192 The CP-violating form factor F_3 is associated with the EDM of the lepton d_f through

$$d_f = \frac{e F_3^{(f)}(0)}{2 m_f}. \quad (5.19)$$

193 In the SM, d_f starts to receive contributions at three loops for quarks [39] and at four loops
 194 for leptons [40], induced by the CP violation in the CKM matrix. For protons and neutrons
 195 there is an additional source for an EDM [41] through the CP-violating θ term in QCD

$$\mathcal{L}_{\text{QCD}} \supset \frac{g_s^2 \theta}{32 \pi^2} \tilde{G}_{\alpha\beta} G^{\alpha\beta}, \quad (5.20)$$

196 which we have neglected in (5.1). This term has to be included as it respects $SU(3)_c$ gauge
 197 invariance. Even though it can be written as a total derivative and, so does not affect the
 198 classical equations of motion, the θ term does have effects at the quantum level. Thus strong
 199 interactions seem to violate CP. However, due to experimental constraints on the neutron EDM,
 200 we know that the θ parameter is extremely small, see Section 5.6. The lack of an explanation
 201 for this smallness is referred to as the strong CP problem. In generic BSM models, one usually
 202 expects much larger CP-violating effects [42, 43]. The parity-violating anapole form factor F_4 is
 203 also induced due to weak interactions of the SM, or potentially through BSM effects. However,
 204 it is not an observable by itself [44].

205 As mentioned above, matrix elements of the weak charged current J_{cc}^α also play an impor-
 206 tant role. It gives rise to non-vanishing matrix elements between different particles of left-
 207 handed $SU(2)$ doublets, such as (ν_ℓ, ℓ) or (p, n) . The former leads to muon decay, whereas
 208 the latter for example to beta decay, or quasi-elastic scattering $\ell p \rightarrow \nu_\ell n$. In this case, all six
 209 structures appear and setting $m_p = m_n \equiv m_N$ we have

$$\begin{aligned} \langle p(p_2) | J_{\text{cc}}^\alpha | n(p_1) \rangle = & \bar{u}(p_2, m_N) \left(F_1^{(pn)}(q^2) \gamma^\alpha + F_2^{(pn)}(q^2) \frac{i \sigma^{\alpha\beta} q_\beta}{2 m_N} + F_A^{(pn)}(q^2) \gamma^\alpha \gamma_5 \right. \\ & \left. + F_P^{(pn)}(q^2) \frac{q^\alpha \gamma_5}{2 m_N} + F_S^{(pn)}(q^2) \frac{q^\alpha}{m_N} + F_T^{(pn)}(q^2) \frac{i \sigma^{\alpha\beta} q_\beta \gamma_5}{2 m_N} \right) u(p_1, m_N). \end{aligned} \quad (5.21)$$

210 The scalar and tensor form factors F_S and F_T are referred to as second-class currents and often
 211 are omitted. However, we will return to them in Section 5.6 in connection with the nucleon
 212 β^- decay, see (5.48), which can be related to $F_{S,T}^{(pn)}$ and $F_{S,T}^{(\nu_e e^-)}$. The axial-vector and the
 213 pseudoscalar form factors, $F_A^{(pn)}$, and $F_P^{(pn)}$ are related to often used couplings as

$$g_A \equiv F_A^{(pn)}(0), \quad \bar{g}_A \equiv F_A^{(pn)}(q_0^2), \quad \bar{g}_P \equiv \frac{m_\mu}{m_N} F_P^{(pn)}(q_0^2), \quad (5.22)$$

214 where $q_0^2 = -0.88 m_\mu^2$ is the momentum transfer of μ^- capture on the proton, neglecting
 215 binding energies.

216 5.2.3 Hadronic effects

217 Not only the Wilson coefficients of the EFTs are subject to RGEs and thus scale dependent, but
 218 also the gauge couplings $\alpha = e^2/(4\pi)$ and $\alpha_s = g_s^2/(4\pi)$ in (5.1). Both depend on the energy of
 219 the phenomenon they are used to describe, but while $\alpha(Q^2)$ decreases towards $\alpha(0) \sim 1/137$,
 220 the strong coupling $\alpha_s(Q^2)$ increases as we go to lower energies. For energy scales below a cou-
 221 ple of GeV, a perturbative expansion in α_s no longer works — the relevant degrees of freedom
 222 related to the strong interactions at low energies are not quarks and gluons, but light hadrons.
 223 Once more, EFTs come to the rescue, in this case chiral perturbation theory (χ PT) [45–47].
 224 As for all EFTs, the first step is to identify the relevant degrees of freedom in the energy range
 225 of interest. The second is to write down the most general Lagrangian for these degrees of
 226 freedom that is compatible with the symmetries of the underlying theory. For the strong in-
 227 teractions the answer to the first question is related to the phenomenon of spontaneous chiral
 228 symmetry breaking, which generates Goldstone bosons, the only massless particles of strong
 229 interactions. Actually in the spectrum of QCD there are no massless particles, but a triplet
 230 of very light pseudoscalars, the pions $\vec{\pi} = (\pi^+, \pi^0, \pi^-)$. The fact that they are not exactly
 231 massless is well understood and due to the presence of an explicit, but small, chiral symmetry
 232 breaking term in the QCD Lagrangian: the quark mass term. In the limit of zero up and down
 233 quark masses, i.e., $m_d = m_u = 0$, the three pions become massless, and since there are no
 234 other mechanisms to generate massless particles in QCD in the chiral limit, these are the only
 235 relevant degrees of freedom at low energy.

236 The rules to write down an effective Lagrangian for Goldstone bosons are well known.
 237 Goldstone bosons transform nonlinearly under the symmetry of the underlying theory, which
 238 leads to a non-renormalizable Lagrangian containing only derivative couplings. Symmetry
 239 constrains their interaction to become weaker as one lowers the energy. How to include an
 240 explicit symmetry breaking is also well known. The symmetry breaking parameters are pro-
 241 moted to spurions, fields with given transformation laws, and the effective Lagrangian must
 242 include these fields too and still satisfy the requirement of being invariant under symmetry
 243 transformations. In the case of QCD, in addition to derivative couplings, it is also possible to
 244 have couplings proportional to the quark masses $m_{u,d}$. Clearly, there are infinitely many such
 245 terms and the Lagrangian only becomes useful with an organizing principle. Since this is a
 246 low-energy EFT, we count powers of energy or momenta as small, and since it is relativistic,
 247 they come in even powers. The smallest possible number is two, then four, six and so on.
 248 Quark masses (or explicit symmetry breaking in general) also count as small, but there is no
 249 unique choice concerning the relative importance of powers of quark masses and derivatives.
 250 The standard one is $m \sim p^2$. According to this choice the lowest-order Lagrangian contains all
 251 possible terms with two powers of derivatives or one power of quark masses and it turns out
 252 that there are only two:

$$\mathcal{L}_{\chi\text{PT}} = \mathcal{L}_2 + \mathcal{L}_4 + \mathcal{L}_6 + \dots, \quad \mathcal{L}_2 = \frac{F^2}{4} \langle u_\mu u^\mu + \chi_+ \rangle, \quad (5.23)$$

253 where $u_\mu = iu^\dagger \partial_\mu U u^\dagger$, $\chi_+ = u^\dagger \chi u^\dagger + u \chi^\dagger u$, and

$$U = uu = \exp(i\phi/F), \quad \phi = \pi^a \tau_a, \quad \chi = 2B \text{diag}(m_u, m_d), \quad (5.24)$$

254 with π^a the triplet of pion fields and τ_a the Pauli matrices. The low-energy constant (LEC) F
255 is related to the pion decay constant

$$\langle 0 | (J_A^a)_\mu(0) | \pi^b(p) \rangle = i\delta^{ab} F_\pi p_\mu, \quad F_\pi = F(1 + \mathcal{O}(m_q)), \quad (5.25)$$

256 with $(J_A^a)_\mu$ the isospin-triplet axial current. The second LEC B is defined through the quark
257 condensate in the chiral limit,

$$B = -\frac{\langle 0 | \bar{u}u | 0 \rangle}{F^2} = -\frac{\langle 0 | \bar{d}d | 0 \rangle}{F^2}, \quad (5.26)$$

258 and also relates the pion mass to the quark mass according to the Gell-Mann–Oakes–Renner
259 relation [48]

$$m_\pi^2 = 2B\hat{m}(1 + \mathcal{O}(m_q)), \quad (5.27)$$

260 with $\hat{m} = (m_u + m_d)/2$. Calculating tree-level diagrams with \mathcal{L}_2 gives a leading-order (LO)
261 result. Going to next-to-leading order (NLO) requires calculating one-loop diagrams with ver-
262 tices only from \mathcal{L}_2 and tree-level diagrams with one vertex from \mathcal{L}_4 [32, 46]. At next-to-next-to-
263 leading order (NNLO) two-loop diagrams with vertices only from \mathcal{L}_2 , one-loop diagrams with
264 one vertex from \mathcal{L}_4 and tree-level diagrams with two vertices from \mathcal{L}_4 or one from \mathcal{L}_6 con-
265 tribute [49–51], and so on.

266 The limit of validity of this EFT is given by the scale of chiral symmetry breaking. In
267 the expansion in powers of momenta and quark masses that is generated by the effective
268 Lagrangian above, the relevant scale is represented by $\Lambda_\chi = 4\pi F_\pi \sim 1.2$ GeV. Physically it
269 represents the scale at which degrees of freedom other than Goldstone bosons get excited,
270 such as the ρ , whose mass $m_\rho \sim 0.77$ GeV is indeed close to Λ_χ .

271 The same approach also works for other particles beyond the pions. In the limit $m_s \rightarrow 0$
272 also the kaons and the eta become Goldstone bosons and can be included in the formalism
273 above [52]. The field ϕ becomes a 3×3 matrix containing the octet of Goldstone bosons
274 $\phi = \phi^a \lambda_a$, and χ has to be trivially extended to a diagonal 3×3 quark-mass matrix.

275 A less trivial extension concerns the baryon sector [53–56]. At first sight this would seem
276 impossible, since the mass of the nucleons is close to Λ_χ . But the baryon number n_B is con-
277 served in strong interactions and one can split the spectrum in separated sectors, labeled by
278 n_B . Quantities like the nucleon masses, their form factors, or their scattering amplitude with a
279 pion (or any other Goldstone boson(s)) all belong to the sector $n_B = 1$ and can also be studied
280 with the help of the chiral expansion. In this case this represents an expansion in powers of
281 momenta and quark masses around the ground-state energy, which in this sector is equal to
282 the mass of the nucleon m_N , rather than zero.

283 From the point of view of their transformation properties, nucleons are spin-1/2 as well
284 as isospin-1/2 particles, and transform linearly under chiral transformations. In particular the
285 fact that they are spin-1/2 particles has an important consequence as the expansion of the
286 Lagrangian in powers of momenta (derivatives) contains both even and odd powers

$$\mathcal{L}_N = \mathcal{L}_1 + \mathcal{L}_2 + \mathcal{L}_3 + \dots \quad (5.28)$$

287 The leading-order Lagrangian looks as follows

$$\mathcal{L}_1 = \bar{N}(i\not{D} - m)N + \frac{1}{2}g_A \bar{N} \not{\psi} \gamma_5 N \quad (5.29)$$

288 with the covariant derivative defined as

$$D_\mu = \partial_\mu + \Gamma_\mu, \quad \Gamma_\mu = \frac{1}{2}[u^\dagger, \partial_\mu u], \quad (5.30)$$

289 and $\bar{N} = (\bar{p}, \bar{n})$ the isospin doublet containing the Dirac spinors of the proton and neutron. The
 290 parameters m and g_A represent the mass and the axial coupling of the nucleon in the chiral
 291 limit, respectively. Note that the chiral symmetry imposes the presence of the pion field both
 292 in the covariant derivative as well as in the coupling to the nucleon axial current. From this
 293 follows the famous Golberger-Treiman relation [57]

$$g_{\pi N} = \frac{g_A m_N}{F_\pi} \quad (5.31)$$

294 between the pion-nucleon coupling constant $g_{\pi N}$ (whose square is the residue of the nucleon
 295 pole in the πN scattering amplitude), the physical nucleon mass, and the axial coupling.

296 The low-energy description of the strong-interaction effects in terms of χ PT cannot only
 297 be formulated for pure QCD as the underlying theory. While QED effects can be included in
 298 terms of explicit low-energy degrees of freedom, the chiral realization of higher-dimensional
 299 operators again is based on the external-field and spurion technique. Traditionally, this has
 300 been done to include weak-interaction effects and it can be generalized to include BSM effects
 301 encoded in the LEFT Lagrangian (5.16).

302 5.3 The muon

303 The muon is a fundamental lepton similar to the electron, however with a much larger mass,
 304 $m_\mu \simeq 105.66 \text{ MeV}$. It is unstable and predominantly decays through the Michel process

$$\mu \rightarrow e \nu \bar{\nu}, \quad (5.32)$$

305 which leads² to a lifetime of about $\tau_\mu \simeq 2.2 \mu\text{s}$. As discussed in the context of (5.21) the decay
 306 is mediated by the charged current J_{cc}^α , leading to a non-vanishing current-current interaction
 307 $\langle \nu_\mu | J_{\text{cc}}^\alpha | \mu \rangle \langle e | (J_{\text{cc}}^\alpha)^\dagger | \nu_e \rangle$. From an EFT point of view this corresponds to a four-fermion oper-
 308 ator $(\bar{\nu}_\mu \gamma^\alpha P_L \mu)(\bar{e} \gamma_\alpha P_L \nu_e)$ and its Hermitian conjugate. For computational reasons it is more
 309 convenient to work with the Fierz transform of this operator. This results in the Fermi theory,
 310 an EFT defined through the Lagrangian

$$\mathcal{L}_{\text{Fermi}} = -\frac{4G_F}{\sqrt{2}} (\bar{\nu}_\mu \gamma_\alpha P_L \nu_e)(\bar{e} \gamma^\alpha P_L \mu) + \text{h.c.} + \mathcal{L}_{\text{QED+QCD}}, \quad (5.33)$$

311 where it is implicitly assumed that only light quarks are included in \mathcal{L}_{QCD} . The first term on
 312 the r.h.s. of (5.33) corresponds to the operator $[O_{\nu\ell}^{V,LL}]_{2112}$ as introduced in (5.12). Its Wilson
 313 coefficient, $4G_F/\sqrt{2}$, has the special property that it does not get renormalized [58]. Thus,
 314 the Lagrangian (5.33) can be used to consistently compute at leading order in G_F but to all
 315 orders in the electromagnetic coupling α . Only the usual QED renormalization procedure has
 316 to be applied. As an example, the lifetime of the muon can be expressed as

$$\frac{1}{\tau_\mu} \equiv \Gamma_\mu = \Gamma_0(1 + \Delta q) = \frac{G_F^2 m_\mu^5}{192 \pi^3} (1 + \Delta q), \quad (5.34)$$

317 where Δq contains all corrections to Γ_0 (the tree-level result for massless electrons) that are
 318 induced by (5.33). This includes electron-mass effects, higher-order QED corrections, as well

² Section 16: MuLan [2]

319 as hadronic corrections. While the former two can be computed in perturbation theory, the
 320 latter are more delicate. As mentioned above, QCD is non-perturbative at scales typical for
 321 muonic processes, $q^2 \sim m_\mu^2$. Thus, the hadronic contributions have to be determined by other
 322 means. This is often the leading theoretical uncertainty. The fact that such corrections for
 323 muonic processes enter only at NNLO makes the muon a rather clean laboratory for precision
 324 physics. Typically, \mathcal{L}_{QED} contains muon and electron fields, but the inclusion of τ leptons is
 325 straightforward, as is the inclusion of heavy quarks in \mathcal{L}_{QCD} .

326 The corrections Δq are known at NNLO with full electron mass dependence [59–62]. Thus,
 327 with a precision measurement of the muon lifetime, the Wilson coefficient in (5.33), or equiv-
 328 alently G_F , can be determined extremely precisely. This, in turn, is an important input for
 329 electroweak precision tests. In fact, G_F can be related to m_W and m_Z through

$$\frac{4G_F}{\sqrt{2}} = \frac{g^2}{2m_W^2} (1 + \Delta r) = \frac{2\pi\alpha}{\sin^2\theta_W m_W^2} (1 + \Delta r), \quad (5.35)$$

330 where (in the on-shell scheme) $\sin^2\theta_W = 1 - m_W^2/m_Z^2$. The SM corrections Δr contain (par-
 331 tially hadronic) fermion loop contributions to the charge renormalization. Additional con-
 332 tributions depend also on the top and Higgs mass. This makes G_F a decisive input for SM
 333 consistency checks. As mentioned in [2] only the availability of the NNLO result [59] allowed
 334 for a full exploitation of the experimental results.

335 While SM corrections are crucial for the electroweak precision tests the tree-level matching
 336 of the SM to the Fermi theory yields the matching condition (5.35) with $\Delta r \rightarrow 0$ that is used
 337 in (5.33). Furthermore, terms of order q^2/m_W^2 relative to the four-fermion interaction are also
 338 neglected in (5.33) and typically in (5.16). In the literature (5.34) is often written with an
 339 additional factor $(1 + 3/5(m_\mu/m_W)^2)$ which results in a 10^{-6} correction. Within the EFT, such
 340 corrections are reproduced by dimension-8 operators, which are missing in (5.33). There are
 341 also numerous dimension-6 operators generated by the SM that are not included in (5.33). The
 342 corresponding Wilson coefficients are related to the general parametrization of muon decay
 343 parameters.¹

344 Apart from the Michel decay, two further SM decay processes are of interest; the radiative
 345 and rare decays

$$\mu \rightarrow e\nu\bar{\nu}\gamma, \quad \mu \rightarrow e\nu\bar{\nu}e^+e^-. \quad (5.36)$$

346 In order to be well defined and to avoid infrared singularities, the branching ratio for the radi-
 347 ative decay must be defined requiring a minimal energy of the photon. For $E_\gamma > 10$ MeV we have
 348 $B(\mu \rightarrow e\nu\bar{\nu}\gamma) \sim 1.3 \times 10^{-2}$. For the rare decay the branching ratio is $B(\mu \rightarrow e\nu\bar{\nu}ee) \sim 3.6 \times 10^{-5}$.
 349 A fully differential NLO description of these processes in the Fermi theory (5.33) is avail-
 350 able [63–66]. Depending on the cuts that are applied, the NLO QED corrections can be size-
 351 able. Experimental information on the branching ratio of the radiative decay has been obtained
 352 by MEG [67] and PiBeta [68].

353 A particularly attractive feature of particle physics with muons is the study of cLFV decays.
 354 There are three "golden" channels

$$\mu \rightarrow e\gamma, \quad \mu \rightarrow eee, \quad \mu^- \xrightarrow{\Lambda} e^- \xrightarrow{\Lambda} N. \quad (5.37)$$

355 PSI has a long tradition in corresponding experimental searches.^{3,4,5,6} For the first two pro-
 356 cesses typically μ^+ are used, whereas μ^- must be used for muon conversion in the field of a

³ Section 7: SINDRUM [3]

⁴ Section 8: SINDRUM II [4]

⁵ Section 19: MEG [5]

⁶ Section 20: Mu3e [6]

357 nucleus ${}^A_Z N$ with atomic number Z and mass number A . In the SM (with non-vanishing neu-
 358 trino masses) the branching ratios for these processes are smaller than 10^{-50} , but not zero [69].
 359 Hence, from a theory point of view there is nothing sacred about lepton flavor. As we know
 360 that it is not conserved, it is very natural to expect much larger cLFV branching ratios in BSM
 361 than in the SM. In fact, generic extensions of the SM do typically lead to large cLFV rates and
 362 suppressing them requires additional tuning or model-building efforts.

363 To extract constraints on BSM physics from limits on the branching ratios of the processes
 364 (5.37), they are computed in $\mathcal{L}_{\text{LEFT}}$, typically at tree level. For $\mu \rightarrow e\gamma$ the dipole operator
 365 $[O_{\ell\gamma}^D]_{21}$ (5.14) enters. Thus we get a limit on the corresponding Wilson coefficient at the
 366 low scale $[C_{\ell\gamma}^D]_{21}(m_\mu)$. In a next step, the RGE is used to convert this to limits for the Wilson
 367 coefficients at the high scale, $C_i(\Lambda)$. Some scalar four-fermion interactions mix at NLO whereas
 368 vector four-fermion interactions enter at NNLO. Nevertheless, this results in very stringent
 369 limits on contact interactions induced by BSM physics. They have to be combined with limits
 370 from $\mu \rightarrow eee$ and muon conversion, where contact interactions already appear at leading
 371 order. Using as many operators as possible in connection with RGE maximises the information
 372 that can be obtained from low-energy observables.

373 These computations can be made [70] for $\mu \rightarrow e\gamma$ and $\mu \rightarrow eee$ using standard perturba-
 374 tive methods with the Lagrangian (5.16), although for some contributions, non-perturbative
 375 effects play a role [71]. However, additional input is required for muon conversion. First, the
 376 nuclear matrix elements $\langle {}^A_Z N | J | {}^A_Z N \rangle$ for vector and scalar currents/operators are required. The
 377 former can be obtained trivially through current conversion, but the latter need input from
 378 lattice QCD or χ PT. Second, the overlap integrals of the lepton wave function with the nucleus
 379 are required [72]. In principle different target nuclei provide different limits on the various
 380 coefficients, but in practice the model discriminating power is limited [73]. A further compli-
 381 cation is due to background from the decay in orbit (DIO). This is the Michel decay of the μ^-
 382 bound in the nucleus

$$\mu^- {}^A_Z N \rightarrow e^- \nu_\mu \bar{\nu}_e {}^A_Z N. \quad (5.38)$$

383 Due to nuclear recoil effects the energy spectrum of the electron has a tail up to m_μ , the
 384 energy of the signal for the electron from muon conversion. Thus DIO has to be studied as a
 385 background process [74].

386 So far the nucleus has acted only as a spectator. The only nuclear physics that was required
 387 is the nuclear matrix element. For completeness we mention here two processes relevant to
 388 muon conversion, where the nuclear physics is much more involved. When the μ^- is bound to
 389 the nucleus, it quickly cascades to the 1S ground state. Then it might undergo muon capture

$$\mu^- {}^A_Z N \rightarrow \nu_\mu {}^A_{Z-1} N \quad (5.39)$$

390 before it decays. The corresponding nuclear matrix element $\langle {}^A_{Z-1} N | (J_{cc}^\alpha)^\dagger | {}^A_Z N \rangle$ is an extended
 391 version of (5.21). It depends on the details of ${}^A_Z N$ and is not easily accessible with theoretical
 392 methods. We will return to muon capture in Section 5.4.

393 The muon can not only form bound states with a nucleus, but also with an electron. Muo-
 394 nium, $M = (\mu^+ e^-)$, is a bound state like hydrogen, but with the proton replaced by a positive
 395 muon. As the latter is a pointlike fermion, muonium is an excellent laboratory for QED tests,
 396 and for a precise determination of the muon mass.⁷ As the muonium mass is dominated by
 397 antimatter, M is also an interesting option to study experimentally gravity of antimatter [75].
 398 In addition, muonium-antimuonium oscillations

$$M = (\mu^+ e^-) \leftrightarrow \bar{M} = (\mu^- e^+), \quad (5.40)$$

⁷ Section 29: MSpec, Mu-Mass [7]

399 which are forbidden in the SM, are another channel to scrutinize BSM physics.⁸ A bound state
400 of two muons, true muonium ($\mu^+\mu^-$), is unfortunately, not experimentally accessible in the
401 foreseeable future.

402 Two further properties of the muon that are of utmost importance are the AMM (5.4) and
403 EDM (5.19). The motivation to study them in detail is again driven by the desire to test the
404 SM. For the AMM very precise measurements are confronted with similarly precise theoretical
405 predictions [76]. At the time of writing, there is an intriguing tension between SM theory and
406 experiment. For the EDM, the situation is similar to cLFV searches in that the SM value is
407 zero for practical experimental purposes. Hence, experimental verification of a non-vanishing
408 muon EDM is a clear indication of BSM. So far, these quantities have not been measured by PSI
409 experiments. However, future involvement, in particular for the EDM, is being considered [77].

410 5.4 The proton

411 Like the electron and muon, the proton is a charged spin 1/2 fermion. However, because the
412 proton is a bound state, the form factors (5.5) cannot be computed perturbatively simply using
413 $\mathcal{L}_{\text{QED+QCD}}$. Most information is obtained from experiment, with additional input from lattice
414 QCD and χ PT [78]. From the charge and measurements of the AMM we know $F_1^{(p)}(0) = 1$
415 and $F_2^{(p)}(0) = \kappa_p \simeq 1.79$.

416 A quantity that has received a lot of attention in the past years is the proton charge radius
417 $r_E^{(p)}$. As discussed in the context of (5.8), the radius can be extracted as the slope of $G_E^{(p)}(q^2)$
418 at $q^2 \rightarrow 0$. This can be determined by low- q^2 lepton-proton scattering with a careful $q^2 \rightarrow 0$
419 extrapolation. An alternative approach is to use spectroscopy of normal hydrogen or better
420 muonic hydrogen. The overlap of the lepton wave function with the proton charge distribution
421 impacts on the energy levels. Thus, a precise measurement of different transition energies
422 allows the extraction of information on the proton radius. As the Bohr radius is proportional
423 to $1/m_\ell$, the effect in muonic atoms is considerably larger. This has resulted in a very precise
424 new determination of the proton radius⁹ and a new world average of $r_E^{(p)} \simeq 0.84$ fm. The
425 disagreement with earlier determinations of $r_E^{(p)}$ was referred to as proton radius puzzle [79,
426 80], but the puzzle is fading away [81].

427 The CREMA collaboration⁹ has measured two transition frequencies for muonic hydro-
428 gen; the triplet $E(2P_{3/2}^{F=2}) - E(2S_{1/2}^{F=1})$ and singlet $E(2P_{3/2}^{F=1}) - E(2S_{1/2}^{F=0})$. From these two
429 values and theoretical input for the fine structure, it is possible to extract the Lamb shift
430 $E_L = E(2P_{1/2}) - E(2S_{1/2})$ and the hyperfine splitting $E_{HFS} = E(2S_{1/2}^{F=1}) - E(2S_{1/2}^{F=0})$. The
431 discrepancy of the proton radius determination from muonic hydrogen with earlier values
432 initiated a flurry of activities to revisit the theoretical calculations of the energy levels, as sum-
433 marized in [82]. This involves radiative corrections and recoil effects, which can in principle
434 be computed in perturbation theory.

435 In addition there are proton-structure effects, which are divided into two categories: a)
436 finite-size effects, which depend on the charge ρ_E and magnetic moment distribution ρ_M of
437 the proton, i.e., the charges related to the form factors $G_E^{(p)}$ and $G_M^{(p)}$, introduced in (5.6); b)
438 polarizability effects.

439 The leading finite-size effect for E_L is in fact proportional to $(r_E^{(p)})^2$ and it is precisely
440 this effect that allows an accurate determination of $r_E^{(p)}$ from muonic hydrogen spectroscopy
441 to be made. There are also higher-order effects which have to be included, most notably a

⁸ Section 9: MACS [8]

⁹ Section 21: CREMA [9]

442 contribution from the so-called third Zemach moment

$$(r_F^{(p)})^3 \equiv \frac{48}{\pi} \int_0^\infty \frac{dQ}{Q^4} \left([G_E^{(p)}(Q^2)]^2 - 1 + \frac{1}{3} [r_E^{(p)}]^2 Q^2 \right), \quad (5.41)$$

443 where $r_F^{(p)}$ is referred to as Friar radius. This contribution is related to the elastic two-photon
 444 exchange (TPE), where elastic refers to the fact that the intermediate hadronic state is still a
 445 proton. The inelastic TPE, i.e., TPE where the intermediate hadronic state is more complicated,
 446 is often referred to as polarizability correction.

447 A similar distinction between perturbative and finite-size contributions can be made for the
 448 hyperfine splitting E_{HFS} . In this case, the leading finite-size effect is proportional to the Zemach
 449 radius $r_Z^{(p)} \simeq 1.0$ fm, a convolution of the charge distribution with the magnetic moment
 450 distribution

$$r_Z^{(p)} \equiv \int d^3\vec{r}_1 \int d^3\vec{r}_2 \rho_E^{(p)}(\vec{r}_1) \rho_M^{(p)}(\vec{r}_2) |\vec{r}_1 - \vec{r}_2|. \quad (5.42)$$

451 While the determination of the magnetic radius of the proton $r_M^{(p)} \simeq 0.8$ fm was discussed
 452 less controversially, there is also quite a spread in the values obtained from different extrac-
 453 tions [83]. This spread is typically attributed to different treatment of TPE contributions.

454 The CREMA collaboration also investigated muonic deuterium and helium⁹ and deter-
 455 mined the corresponding charge radii. Measuring the charge radii of higher Z nuclei¹⁰ pro-
 456 vides crucial input for potential atomic parity violation experiments.

457 Returning to the proton, as mentioned above, studying lepton-proton scattering at low q^2
 458 is an important source to obtain information on the proton form factors and, hence, the proton
 459 radius. At tree level, which implies the one-photon approximation, this process is described
 460 by the famous Rosenbluth formula

$$\frac{d\sigma}{d\Omega} = \frac{\alpha^2}{4E_1^2 \sin^4 \theta_2} \frac{E_3}{E_1} \left(\frac{[G_E^{(p)}(q^2)]^2 + \tau [G_M^{(p)}(q^2)]^2}{1 + \tau} \cos^2 \theta_2 + 2\tau [G_M^{(p)}(q^2)]^2 \sin^2 \theta_2 \right) \quad (5.43)$$

461 in terms of $\tau = -q^2/(4m_p^2)$, the scattering angle $\theta = 2\theta_2$, and the energies of the incoming
 462 and outgoing leptons, E_1 and E_3 , respectively. Using the standard dipole form $G_D(q^2)$ for the
 463 form factors gives a good fit to the experimental data:

$$G_E^{(p)}(q^2) \simeq \frac{G_M^{(p)}(q^2)}{1 + \kappa_p} \simeq G_D(q^2) = \frac{1}{(1 - q^2/\Lambda^2)^2} \quad \text{with } \Lambda^2 = 0.71 \text{ GeV}^2. \quad (5.44)$$

464 For very small q^2 the form factors deviate from (5.44) and — coming back to the proton radius
 465 issue — it is a delicate problem to extract the slope of the form factors in the limit $q^2 \rightarrow 0$ from
 466 scattering data.

467 Given the importance of lepton-proton scattering, there is a vast literature on the compu-
 468 tation of higher-order corrections to (5.43). These corrections can be split into gauge inde-
 469 pendent and finite subsets by separately considering radiative corrections from the lepton line,
 470 radiation from the proton line, and multi-photon exchange between the proton and electron.

471 A full NLO calculation, superseding earlier ones where various approximations had been
 472 used, has been presented in [84] and there are several Monte Carlo generators with these
 473 corrections implemented [85, 86]. Corrections at NNLO due to radiation from the electron
 474 line have also been computed [87, 88]. Due to the small mass of the lepton, these are the

¹⁰ Section 22: muX [10]

475 dominant corrections, particularly for electron-proton scattering. As for spectroscopy, from a
 476 theoretical point of view, multi-photon exchange contributions between the lepton and proton
 477 are the most difficult ones to handle. Accordingly, TPE contributions have received a lot of
 478 attention, also including the inelastic parts, see e.g. [89–92].

479 Traditionally, these experiments have been carried out with electrons. The MUSE collab-
 480 oration¹¹ proposes to measure $\ell p \rightarrow \ell p$ with $\ell \in \{e^\pm, \mu^\pm\}$. This offers the opportunity to
 481 compare $e p$ and μp scattering within the same experimental setup. In addition, experimen-
 482 tal information on TPE can be obtained by measuring the difference between $\ell^+ p$ and $\ell^- p$
 483 scattering.

484 To the best of our knowledge, the proton is a stable particle and in all processes discussed
 485 so far, has been left intact. A low-energy process that affects the proton much more dramati-
 486 cally is muon capture, $\mu^- p \rightarrow n \nu_\mu$. This process can be described by the transition matrix
 487 element (5.21) as a current-current interaction $\langle \nu_\mu | J_{cc}^\alpha | \mu \rangle \langle n | (J_{cc})^\dagger | p \rangle$. In fact, muon capture
 488 on the proton as measured by MuCap¹² gives valuable information on the corresponding form
 489 factors, in particular \bar{g}_p (5.22) [93]. The inverse process would be related to neutrino-nucleon
 490 scattering. Muon capture on the deuterium has been investigated by MuSun.¹³

491 5.5 Nucleons and nuclei

492 The proton and neutron together form an isospin doublet. They differ by their isospin projec-
 493 tion, $I_3 = +1/2$ and $I_3 = -1/2$, and quark content, uud and udd , respectively. The neutron's
 494 Dirac and Pauli form factors are normalized as $F_1^{(n)}(0) = 0$ and $F_2^{(n)}(0) = \kappa_n \simeq -1.91$. The
 495 former differs from the proton form factor at zero momentum transfer, $F_1^{(p)}(0) = 1$, due to
 496 the vanishing charge of the neutron. Therefore, the electric Sachs form factor of the neutron
 497 cannot be approximated with a dipole form factor (5.44). Instead, the Galster form factor
 498 could be used as a simple parametrization [94]:

$$G_E^{(n)}(q^2) = \frac{q^2 \kappa_n}{4m_n^2 - \eta q^2} G_D(q^2), \quad (5.45)$$

499 with $\eta = 5.6$. Since there are no free neutron targets, one has to rely on scattering off light
 500 nuclei (e.g., ^2H or ^3He) to extract the neutron form factors and polarizabilities. Thereby, few-
 501 nucleon EFTs are needed to separate the neutron from proton and nuclear effects.

502 As highlighted in the previous section, muonic atoms are sensitive to the nuclear structure.
 503 The measurement of the muonic-hydrogen Lamb shift by the CREMA collaboration⁹ allowed
 504 the extraction of the proton root-mean-square charge radius with unprecedented precision.
 505 From the measured the Lamb shifts in μD , $\mu^3\text{He}^+$ and $\mu^4\text{He}^+$ the deuteron, helion and α -
 506 particle charge radii can be extracted. In the future, the ground-state hyperfine splitting of
 507 $\mu^3\text{He}^+$ shall be measured to extract the helion Zemach radius. To extract the different nuclear
 508 radii, precise theory predictions for the energy levels in muonic atoms are needed, see theory
 509 summaries in [95–97]. Among other contributions, one needs the finite-size effects, through
 510 which the different radii enter, and the polarizability effects. For the light muonic atoms,
 511 not only the proton polarizability enters, but also the polarizabilities of the neutron and the
 512 nucleus as a whole. Similar complications arise when going from pionic hydrogen to pionic
 513 deuterium¹⁴ or helium.¹⁵ The nuclear polarizabilities are typically several orders of magni-
 514 tude larger than the nucleon polarizabilities, and thus, more important. Take for instance

¹¹ Section 23: MUSE [11]

¹² Section 17: MuCap [12]

¹³ Section 18: MuSun [13]

¹⁴ Section 14: Pionic hydrogen and deuterium [14]

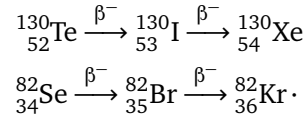
¹⁵ Section 26: Pionic helium [15]

515 the electric dipole polarizability, $\alpha_{E1}^{(n)} = 11.8(1.1) \times 10^{-4} \text{ fm}^3$ [98] and $\alpha_{E1}^{(d)} = 0.6314(19)$
 516 fm^3 [99], which describes the deformation of a composite particle in an external electric field
 517 and gives a dominant contribution to the two-photon exchange. The nuclear polarizability
 518 effects can be calculated in a dispersion relations framework [100, 101] or based on nuclear
 519 potentials. For the latter, one distinguishes calculations with phenomenological models [102]
 520 fit to nucleon-nucleon scattering data, such as the AV18 potential [103], or with nucleon-
 521 nucleon interactions derived from chiral EFT [104–107]. The nucleon-structure contributions
 522 are often deduced by rescaling the proton-structure contributions to μH . Take, for example,
 523 the nucleon-polarizability contribution

$$\delta_{\text{pol}}^{\text{N}}(\mu\text{A}) = (\text{N} + \text{Z}) [Zm_r(\mu\text{A})/m_r(\mu\text{H})]^3 \delta_{\text{pol}}^{\text{N}}(\mu\text{H}), \quad (5.46)$$

524 where m_r is the reduced mass of the muonic atom and Z, N, A are the numbers of protons,
 525 neutrons and nucleons in the nucleus.

526 Also in the field of muonic atoms, the muX project¹⁰ determines nuclear charge radii of
 527 radioactive elements and rare isotopes, e.g., ^{248}Cm and ^{226}Ra , through muonic X-ray measure-
 528 ments. These are needed as input for atomic parity violation experiments. In addition, muX
 529 probes nuclei that are at the end of a double β decay chain. These are interesting in view of
 530 possible neutrinoless double β decay that could occur if neutrinos were Majorana particles.
 531 Two examples are the following $\beta^-\beta^-$ decays:



532 Here one uses muon capture to study excited states of ^{130}Xe and ^{82}Kr . In the future, direct
 533 searches for BSM interactions between muons and nuclei might be possible with the muX
 534 setup.

535 To further advance the precision of the few nucleon EFTs mentioned in this section, the
 536 MuSun experiment¹³ is studying muon-capture on deuterium: $\mu^- d \rightarrow nn\nu_\mu$. The aim is to
 537 determine the LEC of the axial-vector four-nucleon interaction d [108]

$$\mathcal{L}_{NN} = -2d(N^\dagger S \cdot uN)N^\dagger N, \quad (5.47)$$

538 where S^μ is the nucleon covariant spin operator, $N(x)$ is the nucleon field, and u_μ is given
 539 below (5.23). Presently, this LEC has only been extracted from $A = 3$ nuclei. The MuSun
 540 experiment has the potential for an improved extraction at the 20% level.

541 5.6 The free neutron

542 In the previous section, we discussed nuclei and bound neutrons. In the following, we discuss
 543 free neutrons provided by the Swiss Spallation Neutron Source (SINQ) and the PSI Ultra Cold
 544 Neutron (UCN) source [109]. As we will see, the neutron experiments at PSI are dedicated to
 545 BSM searches, and in particular, to the search for CP violation in the light quark sector.

546 The neutron is unstable with a lifetime of about 880 s. The long-standing tension between
 547 measurements with in-flight and stored neutrons has led to speculations that there could be
 548 ‘dark’ BSM decay channels [110, 111]. Within the SM, the neutron decays into the proton,
 549 where the dominant decay channel is the classical β^- decay $n \rightarrow pe^- \bar{\nu}_e$, described by the
 550 current-current interaction from the Fermi theory, (5.11). Besides the dominant $V-A$ structure
 551 of the weak interaction, there could be small admixtures of scalar and tensor couplings. Using
 552 the general formulation of Lee and Yang, which is an older version of the parametrization in

553 (5.21), the β^- decay reads [112]

$$\begin{aligned} \langle pe^- \bar{\nu}_e | n \rangle = & \frac{G_F V_{ud}}{\sqrt{2}} \left[\langle p | n \rangle \langle e^- | C_S - C'_S \gamma_5 | \nu_e \rangle + \langle p | \gamma_\mu | n \rangle \langle e^- | \gamma^\mu (C_V - C'_V \gamma_5) | \nu_e \rangle \right. \\ & + 1/2 \langle p | \sigma_{\lambda\mu} | n \rangle \langle e^- | \sigma^{\lambda\mu} (C_T - C'_T \gamma_5) | \nu_e \rangle - \langle p | \gamma_\mu \gamma_5 | n \rangle \langle e^- | \gamma^\mu \gamma_5 (C_A - C'_A \gamma_5) | \nu_e \rangle \\ & \left. + \langle p | \gamma_5 | n \rangle \langle e^- | \gamma_5 (C_P - C'_P \gamma_5) | \nu_e \rangle + \text{h.c.} \right], \end{aligned} \quad (5.48)$$

554 where $C_i^{(\prime)}$ are 10 complex coupling constants. For the SM with conserved vector current,
555 $g_V = 1$, the only non-vanishing couplings are $C_V = C'_V = 1$ and $C_A = C'_A = -g_A$. Parity
556 violation is assured if $C_i \neq 0$ and $C'_i \neq 0$. Time reversal violation (TRV), or CP violation, is
557 found if $\text{Im}(C_i/C_j) \neq 0$ or $\text{Im}(C'_i/C'_j) \neq 0$, i.e., if at least one coupling has an imaginary phase
558 relative to the others. The nTRV experiment¹⁶ accessed the scalar and tensor couplings through
559 the measurement of the transverse polarization of electrons from the decay of polarized free
560 neutrons. At the present level of precision, the results are in agreement with the SM, thus,
561 setting constraints on BSM physics. For a review on electroweak SM tests with nuclear β
562 decays see [113].

563 The observation of a nonzero permanent EDM of the neutron could be interpreted as a
564 signal of CP violating BSM interactions or a measurement of the QCD θ parameter, see (5.20).
565 The current best limit $|d_n| < 1.8 \times 10^{-26} e \text{ cm}$ is from the nEDM experiment¹⁷ at PSI. This
566 limit is still compatible with the CKM-induced SM contributions to d_n , which are negligible
567 as explained below (5.19). The n2EDM experiment will improve the sensitivity to d_n by an
568 order of magnitude and probe BSM physics at the multi-TeV scale [43]. The electric field
569 of these experiments is of the order of 10^6 V/m . This is well below the critical electric field
570 strength, $E_{\text{crit.}} \sim 10^{23} \text{ V/m}$, that would be able to induce an EDM proportional to the neutron
571 electric dipole polarizability $d_{\text{ind.}} = 4\pi\alpha_{E1} \vec{E}$ [114]. The nEDM spectrometer has also been
572 used in indirect searches for Dark Matter (DM) candidates, e.g., mirror matter or axions and
573 axion-like particles (ALPs).¹⁸

574 5.7 The pion

575 Low-energy pion physics provides access to a large variety of phenomena, ranging from strong
576 non-perturbative dynamics over electroweak precision tests to probes of BSM physics. The
577 pions are stable in pure QCD and as asymptotic QCD states they play a special role in many
578 hadronic processes, where they appear as hadronic final states. Pion interactions can be under-
579 stood beyond the chiral expansion by employing unitarity and analyticity of transition ampli-
580 tudes, which provide a means to resum pion-rescattering effects. Most notably, $\pi\pi$ scattering
581 has been accurately described in terms of the Roy equations [115–117], and the resulting pre-
582 cise determination of the scattering phase shifts provides a central input in the analysis of a
583 host of other hadronic processes at low energies.

584 An important probe of QCD at low energies is provided by the interaction of pions with nu-
585 cleons. Pionic atoms provide access to S -wave πN scattering lengths [118], because the strong
586 interaction changes the spectrum compared to pure QED, resulting in shifts of the energy levels
587 and in finite widths of the bound state. The most precise measurements of pionic hydrogen and
588 deuterium have been performed at PSI.¹⁴ The S -wave scattering lengths enter as important
589 constraints in a dispersive Roy–Steiner analysis of the πN scattering amplitude [119].

¹⁶ Section 15: nTRV [16]

¹⁷ Section 27: nEDM [17]

¹⁸ Section 28: nEDMX [18]

590 Compared to pure strong dynamics in the isospin limit, both electromagnetic effects and
 591 the mass difference between up and down quarks generate small isospin-breaking corrections.
 592 The mass difference of charged and neutral pions is understood to arise almost exclusively
 593 from electromagnetic effects [46, 120, 121]. This mass difference $m_{\pi^-} - m_{\pi^0}$ has been deter-
 594 mined with high precision at PSI¹⁹ starting from $(\pi^- p)$ bound states with subsequent charge-
 595 exchange reaction $\pi^- p \rightarrow \pi^0 n$. m_{π^-} has also been determined at PSI by measuring the energy
 596 spectrum of pionic hydrogen $(\pi^- p)$.²⁰

597 In the presence of electromagnetism, the neutral pion is not a stable particle, and decays
 598 predominantly into two photons. The decay results from the anomalous non-conservation
 599 of the axial current that couples to the pion. Quark-mass and electromagnetic corrections
 600 to the leading Adler–Bell–Jackiw anomaly have been worked out [122, 123]. Further decay
 601 modes, such as $\pi^0 \rightarrow e^+ e^- \gamma$, $\pi^0 \rightarrow 4e$, and $\pi^0 \rightarrow e^+ e^-$ involve the transition $\pi^0 \rightarrow \gamma^* \gamma^{(*)}$ with
 602 one or two virtual photons. The transition form factor for this process has received consid-
 603 erable interest in connection with hadronic contributions to the muon anomalous magnetic
 604 moment [76, 124–126].

605 Charged pions only decay due to the weak interaction. The hadronic part of the decay
 606 rate for $\pi^+ \rightarrow \ell^+ \nu_\ell$ is governed by the pion decay constant F_π of (5.25), whereas the lep-
 607 tonic part results in a helicity suppression by a factor m_ℓ^2 . Hence, the muonic decay mode
 608 dominates over the electronic mode and has been used to measure²¹ the mass of π^+ . Several
 609 other decay modes have been measured at PSI by the SINDRUM,³ PiBeta,²² and PEN²³ experi-
 610 ments, including the radiative decays $\pi^+ \rightarrow \ell^+ \nu_\ell \gamma$ and $\pi^+ \rightarrow e^+ \nu_e e^+ e^-$ and pion beta decay²²
 611 $\pi^+ \rightarrow \pi^0 e^+ \nu_e$. The theoretical description of the radiative decay $\pi^+ \rightarrow \ell^+ \nu_\ell \gamma$ is split into
 612 two parts, the so-called inner bremsstrahlung contributions (IB) and the structure-dependent
 613 terms (SD). The IB consist of the normal pion decay with additional emission of a photon from
 614 the charged external legs. This part depends on F_π . The SD terms require a more involved
 615 parametrization of the QCD effects in terms of two form factors. Apart from an axial form
 616 factor F_A also a vector form factor F_V contributes [127].

617 The charged-pion decays probe the weak interaction in the low-energy regime, where an
 618 excellent description is provided by Fermi’s effective theory of current-current interaction, or
 619 more generally the LEFT framework explained in Section 5.2. The relevant operator is

$$\mathcal{L}_{\text{LEFT}} \supset \sum_{i,j,k,l} C_{vedu}^{V,LL}(\bar{\nu}_i \gamma^\alpha P_L \ell_j)(\bar{d}_k \gamma_\alpha P_L u_l) + \text{h.c.} \quad (5.49)$$

620 with flavor indices i, j, k, l and the SM tree-level matching at the weak scale given by
 621 $C_{vedu}^{V,LL} = -\frac{4G_F}{\sqrt{2}} \delta_{ij} V_{kl}^\dagger$. Therefore, the pion decays probe the CKM matrix element V_{ud} , with
 622 a value of $|V_{ud}| = 0.9739(27)$ resulting from the PiBeta measurement of pion beta decay. Al-
 623 though precise, this value is not competitive with determinations from superallowed nuclear
 624 beta decays [98], which currently are in some tension with first-row CKM unitarity. With the
 625 absence of nuclear structure aspects and with radiative corrections under good theoretical
 626 control [128], pion beta decays are theoretically clean but remain experimentally challenging
 627 due to the tiny branching ratio $\sim 10^{-8}$.

628 Additional semileptonic operators in the LEFT Lagrangian with different Dirac structures
 629 parametrize deviations from the SM and can be probed by several pion decay modes [129].
 630 E.g., strong constraints on the first-generation tensor-operator coefficient $\text{Re}(C_{vedu}^{T,RR})$ arise from
 631 the $\pi^+ \rightarrow e^+ \nu_e \gamma$ Dalitz-plot study of the PiBeta experiment.

¹⁹ Section 12: neutral pions [21]

²⁰ Section 10: negative pions [19]

²¹ Section 11: positive pions [20]

²² Section 24: PiBeta [22]

²³ Section 25: PEN [23]

5.8 Conclusions

Low-energy, high-precision experiments provide essential input to improve our understanding of the fundamental interactions. They complement and extend information obtained from the energy frontier. EFTs are the theoretical tool of choice to describe and interpret their results and indeed they are well suited to describe both the SM and potential deviations therefrom in a model-independent way. In particular it is possible, and crucial, to analyze if potential deviations from the SM in different observables are linked and have a common explanation. There are numerous examples where low-energy constraints rule out apparently attractive new physics scenarios. A broad and vigorous world-wide low-energy experimental program is indispensable to make further progress in testing the SM and searching for physics beyond. Past and future experiments at PSI will continue to play their part in this challenge.

References

- [1] W. Fetscher, *Muon decay*, SciPost Phys. Proc. **2**, ppp (2021), doi:[10.21468/SciPostPhysProc.2.XXX](https://doi.org/10.21468/SciPostPhysProc.2.XXX).
- [2] R. Carey, T. Gorringer and D. Hertzog, *Mulan: a part-per-million measurement of the muon lifetime and determination of the Fermi constant*, SciPost Phys. Proc. **2**, ppp (2021), doi:[10.21468/SciPostPhysProc.2.XXX](https://doi.org/10.21468/SciPostPhysProc.2.XXX).
- [3] R. Eichler and C. Grab, *The SINDRUM-I Experiment*, SciPost Phys. Proc. **2**, ppp (2021), doi:[10.21468/SciPostPhysProc.2.XXX](https://doi.org/10.21468/SciPostPhysProc.2.XXX).
- [4] A. van der Schaaf, *Sindrum II*, SciPost Phys. Proc. **2**, ppp (2021), doi:[10.21468/SciPostPhysProc.2.XXX](https://doi.org/10.21468/SciPostPhysProc.2.XXX).
- [5] A. Baldini and T. Mori, *MEG: Muon to Electron and Gamma*, SciPost Phys. Proc. **2**, ppp (2021), doi:[10.21468/SciPostPhysProc.2.XXX](https://doi.org/10.21468/SciPostPhysProc.2.XXX).
- [6] F. Wauters, *The Mu3e experiment*, SciPost Phys. Proc. **2**, ppp (2021), doi:[10.21468/SciPostPhysProc.2.XXX](https://doi.org/10.21468/SciPostPhysProc.2.XXX).
- [7] B. Ohayon, Z. Burkley and P. Crivelli, *Mspec: Muonium Spectroscopy*, SciPost Phys. Proc. **2**, ppp (2021), doi:[10.21468/SciPostPhysProc.2.XXX](https://doi.org/10.21468/SciPostPhysProc.2.XXX).
- [8] K. Jungmann and L. Willmann, *Muonium-Antimuonium Conversion*, SciPost Phys. Proc. **2**, ppp (2021), doi:[10.21468/SciPostPhysProc.2.XXX](https://doi.org/10.21468/SciPostPhysProc.2.XXX).
- [9] A. Antognini, *crema — t.b.c. ??*, SciPost Phys. Proc. **2**, ppp (2021), doi:[10.21468/SciPostPhysProc.2.XXX](https://doi.org/10.21468/SciPostPhysProc.2.XXX).
- [10] F. Wauters and A. Knecht, *The muX project*, SciPost Phys. Proc. **2**, ppp (2021), doi:[10.21468/SciPostPhysProc.2.XXX](https://doi.org/10.21468/SciPostPhysProc.2.XXX).
- [11] E. Downie, R. Gilman, J. Bernauer and E. Cline, *MUSE: The MUon Scattering Experiment*, SciPost Phys. Proc. **2**, ppp (2021), doi:[10.21468/SciPostPhysProc.2.XXX](https://doi.org/10.21468/SciPostPhysProc.2.XXX).
- [12] M. Hildebrandt and C. Petitjean, *MuCap: Muon Capture on the Proton*, SciPost Phys. Proc. **2**, ppp (2021), doi:[10.21468/SciPostPhysProc.2.XXX](https://doi.org/10.21468/SciPostPhysProc.2.XXX).
- [13] P. Kammel, *MuSun - Muon Capture on the Deuteron*, SciPost Phys. Proc. **2**, ppp (2021), doi:[10.21468/SciPostPhysProc.2.XXX](https://doi.org/10.21468/SciPostPhysProc.2.XXX).

- 671 [14] D. Gotta and L. Simons, *Pionic hydrogen and deuterium*, SciPost Phys. Proc. **2**, ppp
672 (2021), doi:[10.21468/SciPostPhysProc.2.XXX](https://doi.org/10.21468/SciPostPhysProc.2.XXX).
- 673 [15] M. Hori, H. Aghai-Khozani, A. Sótér, A. Dax and D. Barna, *Recent results of laser spec-*
674 *troscopy experiments of pionic helium atoms at PSI*, SciPost Phys. Proc. **2**, ppp (2021),
675 doi:[10.21468/SciPostPhysProc.2.XXX](https://doi.org/10.21468/SciPostPhysProc.2.XXX).
- 676 [16] K. Bodek and A. Kozela, *Measurement of the transverse polarization of electrons*
677 *emitted in neutron decay – nTRV experiment*, SciPost Phys. Proc. **2**, ppp (2021),
678 doi:[10.21468/SciPostPhysProc.2.XXX](https://doi.org/10.21468/SciPostPhysProc.2.XXX).
- 679 [17] G. Pignol and P. Schmidt-Wellenburg, *The search for the neutron electric dipole moment*
680 *at PSI*, SciPost Phys. Proc. **2**, ppp (2021), doi:[10.21468/SciPostPhysProc.2.XXX](https://doi.org/10.21468/SciPostPhysProc.2.XXX).
- 681 [18] S. Roccia and G. Zsigmond, *Indirect searches for dark matter with the nEDM spectrometer*,
682 SciPost Phys. Proc. **2**, ppp (2021), doi:[10.21468/SciPostPhysProc.2.XXX](https://doi.org/10.21468/SciPostPhysProc.2.XXX).
- 683 [19] M. Daum and D. Gotta, *The mass of the π^-* , SciPost Phys. Proc. **2**, ppp (2021),
684 doi:[10.21468/SciPostPhysProc.2.XXX](https://doi.org/10.21468/SciPostPhysProc.2.XXX).
- 685 [20] M. Daum and P-R. Kettle, *The mass of the π^+* , SciPost Phys. Proc. **2**, ppp (2021),
686 doi:[10.21468/SciPostPhysProc.2.XXX](https://doi.org/10.21468/SciPostPhysProc.2.XXX).
- 687 [21] M. Daum and P-R. Kettle, *The π^0 mass and the first experimental verification*
688 *of Coulomb de-excitation in pinoic hydrogen*, SciPost Phys. Proc. **2**, ppp (2021),
689 doi:[10.21468/SciPostPhysProc.2.XXX](https://doi.org/10.21468/SciPostPhysProc.2.XXX).
- 690 [22] D. Pocanic, *The pion beta and radiative electronic decays*, SciPost Phys. Proc. **2**, ppp
691 (2021), doi:[10.21468/SciPostPhysProc.2.XXX](https://doi.org/10.21468/SciPostPhysProc.2.XXX).
- 692 [23] D. Pocanic, *Pion electronic decay and lepton universality*, SciPost Phys. Proc. **2**, ppp
693 (2021), doi:[10.21468/SciPostPhysProc.2.XXX](https://doi.org/10.21468/SciPostPhysProc.2.XXX).
- 694 [24] E. E. Jenkins, A. V. Manohar and P. Stoffer, *Low-Energy Effective Field Theory*
695 *below the Electroweak Scale: Operators and Matching*, JHEP **03**, 016 (2018),
696 doi:[10.1007/JHEP03\(2018\)016](https://doi.org/10.1007/JHEP03(2018)016), [1709.04486](https://arxiv.org/abs/1709.04486).
- 697 [25] R. D. Peccei and H. R. Quinn, *CP Conservation in the Presence of Instantons*, Phys. Rev.
698 Lett. **38**, 1440 (1977), doi:[10.1103/PhysRevLett.38.1440](https://doi.org/10.1103/PhysRevLett.38.1440).
- 699 [26] R. D. Peccei and H. R. Quinn, *Constraints Imposed by CP Conservation in the Presence of*
700 *Instantons*, Phys. Rev. D **16**, 1791 (1977), doi:[10.1103/PhysRevD.16.1791](https://doi.org/10.1103/PhysRevD.16.1791).
- 701 [27] F. Wilczek and A. Zee, *Instantons and Spin Forces Between Massive Quarks*, Phys. Rev.
702 Lett. **40**, 83 (1978), doi:[10.1103/PhysRevLett.40.83](https://doi.org/10.1103/PhysRevLett.40.83).
- 703 [28] S. Weinberg, *A New Light Boson?*, Phys. Rev. Lett. **40**, 223 (1978),
704 doi:[10.1103/PhysRevLett.40.223](https://doi.org/10.1103/PhysRevLett.40.223).
- 705 [29] L. Michel, *Interaction between four half spin particles and the decay of the μ meson*, Proc.
706 Phys. Soc. **A63**, 514 (1950), doi:[10.1088/0370-1298/63/5/311](https://doi.org/10.1088/0370-1298/63/5/311), [,45(1949)].
- 707 [30] W. Fetscher, H. J. Gerber and K. F. Johnson, *Muon Decay: Complete Determination of*
708 *the Interaction and Comparison with the Standard Model*, Phys. Lett. **B173**, 102 (1986),
709 doi:[10.1016/0370-2693\(86\)91239-6](https://doi.org/10.1016/0370-2693(86)91239-6).

- 710 [31] Y. Kuno and Y. Okada, *Muon decay and physics beyond the standard model*, Rev. Mod.
711 Phys. **73**, 151 (2001), doi:[10.1103/RevModPhys.73.151](https://doi.org/10.1103/RevModPhys.73.151), [hep-ph/9909265](https://arxiv.org/abs/hep-ph/9909265).
- 712 [32] S. Weinberg, *Baryon and Lepton Nonconserving Processes*, Phys. Rev. Lett. **43**, 1566
713 (1979), doi:[10.1103/PhysRevLett.43.1566](https://doi.org/10.1103/PhysRevLett.43.1566).
- 714 [33] B. Grzadkowski, M. Iskrzynski, M. Misiak and J. Rosiek, *Dimension-Six Terms in the*
715 *Standard Model Lagrangian*, JHEP **1010**, 085 (2010), doi:[10.1007/JHEP10\(2010\)085](https://doi.org/10.1007/JHEP10(2010)085),
716 [1008.4884](https://arxiv.org/abs/1008.4884).
- 717 [34] E. E. Jenkins, A. V. Manohar and M. Trott, *Renormalization Group Evolution of the*
718 *Standard Model Dimension Six Operators I: Formalism and lambda Dependence*, JHEP
719 **1310**, 087 (2013), doi:[10.1007/JHEP10\(2013\)087](https://doi.org/10.1007/JHEP10(2013)087), [1308.2627](https://arxiv.org/abs/1308.2627).
- 720 [35] E. E. Jenkins, A. V. Manohar and M. Trott, *Renormalization Group Evolution of the Stan-*
721 *dard Model Dimension Six Operators II: Yukawa Dependence*, JHEP **1401**, 035 (2014),
722 doi:[10.1007/JHEP01\(2014\)035](https://doi.org/10.1007/JHEP01(2014)035), [1310.4838](https://arxiv.org/abs/1310.4838).
- 723 [36] R. Alonso, E. E. Jenkins, A. V. Manohar and M. Trott, *Renormalization Group Evolu-*
724 *tion of the Standard Model Dimension Six Operators III: Gauge Coupling Dependence and*
725 *Phenomenology*, JHEP **1404**, 159 (2014), doi:[10.1007/JHEP04\(2014\)159](https://doi.org/10.1007/JHEP04(2014)159), [1312.2014](https://arxiv.org/abs/1312.2014).
- 726 [37] E. E. Jenkins, A. V. Manohar and P. Stoffer, *Low-Energy Effective Field The-*
727 *ory below the Electroweak Scale: Anomalous Dimensions*, JHEP **01**, 084 (2018),
728 doi:[10.1007/JHEP01\(2018\)084](https://doi.org/10.1007/JHEP01(2018)084), [1711.05270](https://arxiv.org/abs/1711.05270).
- 729 [38] W. Dekens and P. Stoffer, *Low-energy effective field theory below the electroweak scale:*
730 *matching at one loop*, JHEP **10**, 197 (2019), doi:[10.1007/JHEP10\(2019\)197](https://doi.org/10.1007/JHEP10(2019)197), [1908.](https://arxiv.org/abs/1908.05295)
731 [05295](https://arxiv.org/abs/1908.05295).
- 732 [39] A. Czarnecki and B. Krause, *Neutron electric dipole moment in the stan-*
733 *dard model: Valence quark contributions*, Phys. Rev. Lett. **78**, 4339 (1997),
734 doi:[10.1103/PhysRevLett.78.4339](https://doi.org/10.1103/PhysRevLett.78.4339), [hep-ph/9704355](https://arxiv.org/abs/hep-ph/9704355).
- 735 [40] M. E. Pospelov and I. B. Khriplovich, *Electric dipole moment of the W boson and the*
736 *electron in the Kobayashi-Maskawa model*, Sov. J. Nucl. Phys. **53**, 638 (1991).
- 737 [41] M. Pospelov and A. Ritz, *Theta induced electric dipole moment of the neutron via QCD sum*
738 *rules*, Phys. Rev. Lett. **83**, 2526 (1999), doi:[10.1103/PhysRevLett.83.2526](https://doi.org/10.1103/PhysRevLett.83.2526), [hep-ph/](https://arxiv.org/abs/hep-ph/9904483)
739 [9904483](https://arxiv.org/abs/9904483).
- 740 [42] M. Pospelov and A. Ritz, *Electric dipole moments as probes of new physics*, Annals Phys.
741 **318**, 119 (2005), doi:[10.1016/j.aop.2005.04.002](https://doi.org/10.1016/j.aop.2005.04.002), [hep-ph/0504231](https://arxiv.org/abs/hep-ph/0504231).
- 742 [43] J. Engel, M. J. Ramsey-Musolf and U. van Kolck, *Electric Dipole Moments of Nucleons,*
743 *Nuclei, and Atoms: The Standard Model and Beyond*, Prog. Part. Nucl. Phys. **71**, 21
744 (2013), doi:[10.1016/j.pnpnp.2013.03.003](https://doi.org/10.1016/j.pnpnp.2013.03.003), [1303.2371](https://arxiv.org/abs/1303.2371).
- 745 [44] M. J. Musolf and B. R. Holstein, *Observability of the anapole moment and neutrino charge*
746 *radius*, Phys. Rev. D **43**, 2956 (1991), doi:[10.1103/PhysRevD.43.2956](https://doi.org/10.1103/PhysRevD.43.2956).
- 747 [45] S. Weinberg, *Phenomenological Lagrangians*, Physica A **96**(1-2), 327 (1979),
748 doi:[10.1016/0378-4371\(79\)90223-1](https://doi.org/10.1016/0378-4371(79)90223-1).
- 749 [46] J. Gasser and H. Leutwyler, *Chiral Perturbation Theory to One Loop*, Annals Phys. **158**,
750 142 (1984), doi:[10.1016/0003-4916\(84\)90242-2](https://doi.org/10.1016/0003-4916(84)90242-2).

- 751 [47] H. Leutwyler, *On the foundations of chiral perturbation theory*, Annals Phys. **235**, 165
752 (1994), doi:[10.1006/aphy.1994.1094](https://doi.org/10.1006/aphy.1994.1094), [hep-ph/9311274](https://arxiv.org/abs/hep-ph/9311274).
- 753 [48] M. Gell-Mann, R. J. Oakes and B. Renner, *Behavior of current divergences under $SU(3)$
754 $\times SU(3)$* , Phys. Rev. **175**, 2195 (1968), doi:[10.1103/PhysRev.175.2195](https://doi.org/10.1103/PhysRev.175.2195).
- 755 [49] H. W. Fearing and S. Scherer, *Extension of the chiral perturbation theory meson La-
756 grangian to order $p(6)$* , Phys. Rev. D **53**, 315 (1996), doi:[10.1103/PhysRevD.53.315](https://doi.org/10.1103/PhysRevD.53.315),
757 [hep-ph/9408346](https://arxiv.org/abs/hep-ph/9408346).
- 758 [50] J. Bijnens, G. Colangelo and G. Ecker, *Renormalization of chiral perturbation theory to
759 order p^{**6}* , Annals Phys. **280**, 100 (2000), doi:[10.1006/aphy.1999.5982](https://doi.org/10.1006/aphy.1999.5982), [hep-ph/
760 9907333](https://arxiv.org/abs/hep-ph/9907333).
- 761 [51] J. Bijnens, G. Colangelo and G. Ecker, *The Mesonic chiral Lagrangian of order p^{**6} ,*
762 JHEP **02**, 020 (1999), doi:[10.1088/1126-6708/1999/02/020](https://doi.org/10.1088/1126-6708/1999/02/020), [hep-ph/9902437](https://arxiv.org/abs/hep-ph/9902437).
- 763 [52] J. Gasser and H. Leutwyler, *Chiral Perturbation Theory: Expansions in the Mass of the
764 Strange Quark*, Nucl. Phys. B **250**, 465 (1985), doi:[10.1016/0550-3213\(85\)90492-4](https://doi.org/10.1016/0550-3213(85)90492-4).
- 765 [53] J. Gasser, M. E. Sainio and A. Svarc, *Nucleons with Chiral Loops*, Nucl. Phys. B **307**, 779
766 (1988), doi:[10.1016/0550-3213\(88\)90108-3](https://doi.org/10.1016/0550-3213(88)90108-3).
- 767 [54] E. E. Jenkins and A. V. Manohar, *Baryon chiral perturbation theory using a heavy fermion
768 Lagrangian*, Phys. Lett. B **255**, 558 (1991), doi:[10.1016/0370-2693\(91\)90266-S](https://doi.org/10.1016/0370-2693(91)90266-S).
- 769 [55] V. Bernard, N. Kaiser, J. Kambor and U. G. Meissner, *Chiral structure of the nucleon*,
770 Nucl. Phys. B **388**, 315 (1992), doi:[10.1016/0550-3213\(92\)90615-I](https://doi.org/10.1016/0550-3213(92)90615-I).
- 771 [56] T. Becher and H. Leutwyler, *Baryon chiral perturbation theory in manifestly Lorentz
772 invariant form*, Eur. Phys. J. C **9**, 643 (1999), doi:[10.1007/PL00021673](https://doi.org/10.1007/PL00021673), [hep-ph/
773 9901384](https://arxiv.org/abs/hep-ph/9901384).
- 774 [57] M. L. Goldberger and S. B. Treiman, *Conserved Currents in the Theory of Fermi Interac-
775 tions*, Phys. Rev. **110**, 1478 (1958), doi:[10.1103/PhysRev.110.1478](https://doi.org/10.1103/PhysRev.110.1478).
- 776 [58] S. Berman and A. Sirlin, *Some considerations on the radiative correc-
777 tions to muon and neutron decay*, Annals of Physics **20**(1), 20 (1962),
778 doi:[http://dx.doi.org/10.1016/0003-4916\(62\)90114-8](https://dx.doi.org/10.1016/0003-4916(62)90114-8).
- 779 [59] T. van Ritbergen and R. G. Stuart, *Complete two loop quantum electrodynamic con-
780 tributions to the muon lifetime in the Fermi model*, Phys.Rev.Lett. **82**, 488 (1999),
781 doi:[10.1103/PhysRevLett.82.488](https://doi.org/10.1103/PhysRevLett.82.488), [hep-ph/9808283](https://arxiv.org/abs/hep-ph/9808283).
- 782 [60] C. Anastasiou, K. Melnikov and F. Petriello, *The Electron energy spectrum in
783 muon decay through $O(\alpha^{**2})$* , JHEP **0709**, 014 (2007), doi:[10.1088/1126-
784 6708/2007/09/014](https://doi.org/10.1088/1126-6708/2007/09/014), [hep-ph/0505069](https://arxiv.org/abs/hep-ph/0505069).
- 785 [61] A. Pak and A. Czarnecki, *Mass effects in muon and semileptonic $b \rightarrow c$ decays*, Phys. Rev.
786 Lett. **100**, 241807 (2008), doi:[10.1103/PhysRevLett.100.241807](https://doi.org/10.1103/PhysRevLett.100.241807), [0803.0960](https://arxiv.org/abs/0803.0960).
- 787 [62] T. Engel, A. Signer and Y. Ulrich, *A subtraction scheme for massive QED*, JHEP **01**, 085
788 (2020), doi:[10.1007/JHEP01\(2020\)085](https://doi.org/10.1007/JHEP01(2020)085), [JHEP20,085(2020)], [1909.10244](https://arxiv.org/abs/1909.10244).
- 789 [63] M. Fael, L. Mercolli and M. Passera, *Radiative μ and τ leptonic decays at NLO*, JHEP **07**,
790 153 (2015), doi:[10.1007/JHEP07\(2015\)153](https://doi.org/10.1007/JHEP07(2015)153), [1506.03416](https://arxiv.org/abs/1506.03416).

- 791 [64] G. M. Pruna, A. Signer and Y. Ulrich, *Fully differential NLO predictions*
792 *for the radiative decay of muons and taus*, Phys. Lett. **B772**, 452 (2017),
793 doi:[10.1016/j.physletb.2017.07.008](https://doi.org/10.1016/j.physletb.2017.07.008), [1705.03782](https://arxiv.org/abs/1705.03782).
- 794 [65] G. M. Pruna, A. Signer and Y. Ulrich, *Fully differential NLO predictions for the rare muon*
795 *decay*, Phys. Lett. **B765**, 280 (2017), doi:[10.1016/j.physletb.2016.12.039](https://doi.org/10.1016/j.physletb.2016.12.039), [1611.03617](https://arxiv.org/abs/1611.03617).
- 796 [66] M. Fael and C. Greub, *Next-to-leading order prediction for the decay $\mu \rightarrow e(ee)\nu\bar{\nu}$* , JHEP
797 **01**, 084 (2017), doi:[10.1007/JHEP01\(2017\)084](https://doi.org/10.1007/JHEP01(2017)084), [1611.03726](https://arxiv.org/abs/1611.03726).
- 798 [67] A. M. Baldini *et al.*, *Measurement of the radiative decay of polarized muons in the MEG*
799 *experiment*, Eur. Phys. J. **C76**(3), 108 (2016), doi:[10.1140/epjc/s10052-016-3947-6](https://doi.org/10.1140/epjc/s10052-016-3947-6),
800 [1312.3217](https://arxiv.org/abs/1312.3217).
- 801 [68] D. Pocanic *et al.*, *New results in rare allowed muon and pion decays*, Int. J. Mod. Phys.
802 Conf. Ser. **35**, 1460437 (2014), doi:[10.1142/S2010194514604372](https://doi.org/10.1142/S2010194514604372), [1403.7416](https://arxiv.org/abs/1403.7416).
- 803 [69] S. T. Petcov, *The Processes $\mu \rightarrow e + \gamma$, $\mu \rightarrow e + \bar{e}$, $\nu' \rightarrow \nu + \gamma$ in the Weinberg-Salam Model*
804 *with Neutrino Mixing*, Sov. J. Nucl. Phys. **25**, 340 (1977), [Erratum: Sov. J. Nucl. Phys.
805 **25**, 698 (1977), Erratum: Yad. Fiz. **25**, 1336 (1977)].
- 806 [70] A. Crivellin, S. Davidson, G. M. Pruna and A. Signer, *Renormalisation-group improved*
807 *analysis of $\mu \rightarrow e$ processes in a systematic effective-field-theory approach*, JHEP **05**, 117
808 (2017), doi:[10.1007/JHEP05\(2017\)117](https://doi.org/10.1007/JHEP05(2017)117), [1702.03020](https://arxiv.org/abs/1702.03020).
- 809 [71] W. Dekens, E. E. Jenkins, A. V. Manohar and P. Stoffer, *Non-perturbative effects in $\mu \rightarrow e\gamma$* ,
810 JHEP **01**, 088 (2019), doi:[10.1007/JHEP01\(2019\)088](https://doi.org/10.1007/JHEP01(2019)088), [1810.05675](https://arxiv.org/abs/1810.05675).
- 811 [72] R. Kitano, M. Koike and Y. Okada, *Detailed calculation of lepton flavor violating*
812 *muon electron conversion rate for various nuclei*, Phys. Rev. **D66**, 096002 (2002),
813 doi:[10.1103/PhysRevD.76.059902](https://doi.org/10.1103/PhysRevD.76.059902), [10.1103/PhysRevD.66.096002](https://doi.org/10.1103/PhysRevD.66.096002), [Erratum: Phys.
814 Rev.D76,059902(2007)], [hep-ph/0203110](https://arxiv.org/abs/hep-ph/0203110).
- 815 [73] V. Cirigliano, R. Kitano, Y. Okada and P. Tuzon, *On the model discriminating*
816 *power of $\mu \rightarrow e$ conversion in nuclei*, Phys. Rev. **D80**, 013002 (2009),
817 doi:[10.1103/PhysRevD.80.013002](https://doi.org/10.1103/PhysRevD.80.013002), [0904.0957](https://arxiv.org/abs/0904.0957).
- 818 [74] A. Czarnecki, M. Dowling, X. Garcia i Tormo, W. J. Marciano and R. Szafron, *Michel*
819 *decay spectrum for a muon bound to a nucleus*, Phys. Rev. **D90**(9), 093002 (2014),
820 doi:[10.1103/PhysRevD.90.093002](https://doi.org/10.1103/PhysRevD.90.093002), [1406.3575](https://arxiv.org/abs/1406.3575).
- 821 [75] A. Antognini, D. M. Kaplan, K. Kirch, A. Knecht, D. C. Mancini, J. D. Phillips, T. J.
822 Phillips, R. D. Reasenberg, T. J. Roberts and A. Soter, *Studying Antimatter Gravity with*
823 *Muonium*, Atoms **6**(2), 17 (2018), doi:[10.3390/atoms6020017](https://doi.org/10.3390/atoms6020017), [1802.01438](https://arxiv.org/abs/1802.01438).
- 824 [76] T. Aoyama *et al.*, *The anomalous magnetic moment of the muon in the Standard Model*,
825 Phys. Rept. **887**, 1 (2020), doi:[10.1016/j.physrep.2020.07.006](https://doi.org/10.1016/j.physrep.2020.07.006), [2006.04822](https://arxiv.org/abs/2006.04822).
- 826 [77] K. Kirch and P. Schmidt-Wellenburg, *Search for electric dipole moments*, EPJ Web Conf.
827 **234**, 01007 (2020), doi:[10.1051/epjconf/202023401007](https://doi.org/10.1051/epjconf/202023401007), [2003.00717](https://arxiv.org/abs/2003.00717).
- 828 [78] C. F. Perdrisat, V. Punjabi and M. Vanderhaeghen, *Nucleon Electromagnetic Form Factors*,
829 Prog. Part. Nucl. Phys. **59**, 694 (2007), doi:[10.1016/j.pnpnp.2007.05.001](https://doi.org/10.1016/j.pnpnp.2007.05.001), [hep-ph/
830 0612014](https://arxiv.org/abs/hep-ph/0612014).

- 831 [79] R. Pohl, R. Gilman, G. A. Miller and K. Pachucki, *Muonic hydrogen and the proton radius*
832 *puzzle*, *Ann. Rev. Nucl. Part. Sci.* **63**, 175 (2013), doi:[10.1146/annurev-nucl-102212-](https://doi.org/10.1146/annurev-nucl-102212-170627)
833 [170627](https://doi.org/10.1146/annurev-nucl-102212-170627), [1301.0905](https://doi.org/10.1146/annurev-nucl-102212-170627).
- 834 [80] C. E. Carlson, *The Proton Radius Puzzle*, *Prog. Part. Nucl. Phys.* **82**, 59 (2015),
835 doi:[10.1016/j.ppnp.2015.01.002](https://doi.org/10.1016/j.ppnp.2015.01.002), [1502.05314](https://doi.org/10.1016/j.ppnp.2015.01.002).
- 836 [81] H.-W. Hammer and U.-G. Meißner, *The proton radius: From a puzzle to precision*, *Sci.*
837 *Bull.* **65**, 257 (2020), doi:[10.1016/j.scib.2019.12.012](https://doi.org/10.1016/j.scib.2019.12.012), [1912.03881](https://doi.org/10.1016/j.scib.2019.12.012).
- 838 [82] A. Antognini, F. Kottmann, F. Biraben, P. Indelicato, F. Nez and R. Pohl, *Theory of the*
839 *2S-2P Lamb shift and 2S hyperfine splitting in muonic hydrogen*, *Annals Phys.* **331**, 127
840 (2013), doi:[10.1016/j.aop.2012.12.003](https://doi.org/10.1016/j.aop.2012.12.003), [1208.2637](https://doi.org/10.1016/j.aop.2012.12.003).
- 841 [83] J. M. Alarcón, D. W. Higinbotham and C. Weiss, *Precise determination of the proton*
842 *magnetic radius from electron scattering data*, *Phys. Rev. C* **102**(3), 035203 (2020),
843 doi:[10.1103/PhysRevC.102.035203](https://doi.org/10.1103/PhysRevC.102.035203), [2002.05167](https://doi.org/10.1103/PhysRevC.102.035203).
- 844 [84] L. C. Maximon and J. A. Tjon, *Radiative corrections to electron-proton scattering*, *Physical*
845 *Review C* **62**(5) (2000), doi:[10.1103/physrevc.62.054320](https://doi.org/10.1103/physrevc.62.054320).
- 846 [85] A. Gramolin, V. Fadin, A. Feldman, R. Gerasimov, D. Nikolenko, I. Rachek and
847 D. Toporkov, *A new event generator for the elastic scattering of charged leptons on pro-*
848 *tons*, *J. Phys. G* **41**(11), 115001 (2014), doi:[10.1088/0954-3899/41/11/115001](https://doi.org/10.1088/0954-3899/41/11/115001),
849 [1401.2959](https://doi.org/10.1088/0954-3899/41/11/115001).
- 850 [86] I. Akushevich, H. Gao, A. Ilyichev and M. Mezziane, *Radiative corrections beyond the ultra*
851 *relativistic limit in unpolarized ep elastic and Møller scatterings for the PRad Experiment at*
852 *Jefferson Laboratory*, *Eur. Phys. J. A* **51**(1), 1 (2015), doi:[10.1140/epja/i2015-15001-8](https://doi.org/10.1140/epja/i2015-15001-8).
- 853 [87] R.-D. Bucoveanu and H. Spiesberger, *Second-Order Leptonic Radiative Corrections for*
854 *Lepton-Proton Scattering*, *Eur. Phys. J. A* **55**(4), 57 (2019), doi:[10.1140/epja/i2019-](https://doi.org/10.1140/epja/i2019-12727-1)
855 [12727-1](https://doi.org/10.1140/epja/i2019-12727-1), [1811.04970](https://doi.org/10.1140/epja/i2019-12727-1).
- 856 [88] P. Banerjee, T. Engel, A. Signer and Y. Ulrich, *QED at NNLO with McMule*, *SciPost Phys.*
857 **9**, 027 (2020), doi:[10.21468/SciPostPhys.9.2.027](https://doi.org/10.21468/SciPostPhys.9.2.027), [2007.01654](https://doi.org/10.21468/SciPostPhys.9.2.027).
- 858 [89] C. E. Carlson and M. Vanderhaeghen, *Two-Photon Physics in Hadronic Processes*, *Ann.*
859 *Rev. Nucl. Part. Sci.* **57**, 171 (2007), doi:[10.1146/annurev.nucl.57.090506.123116](https://doi.org/10.1146/annurev.nucl.57.090506.123116),
860 [hep-ph/0701272](https://doi.org/10.1146/annurev.nucl.57.090506.123116).
- 861 [90] J. Arrington, P. Blunden and W. Melnitchouk, *Review of two-photon exchange in electron*
862 *scattering*, *Prog. Part. Nucl. Phys.* **66**, 782 (2011), doi:[10.1016/j.ppnp.2011.07.003](https://doi.org/10.1016/j.ppnp.2011.07.003),
863 [1105.0951](https://doi.org/10.1016/j.ppnp.2011.07.003).
- 864 [91] A. Afanasev, P. Blunden, D. Hasell and B. Raue, *Two-photon exchange in*
865 *elastic electron-proton scattering*, *Prog. Part. Nucl. Phys.* **95**, 245 (2017),
866 doi:[10.1016/j.ppnp.2017.03.004](https://doi.org/10.1016/j.ppnp.2017.03.004), [1703.03874](https://doi.org/10.1016/j.ppnp.2017.03.004).
- 867 [92] O. Tomalak, B. Pasquini and M. Vanderhaeghen, *Two-photon exchange contribution to*
868 *elastic e^- -proton scattering: Full dispersive treatment of πN states and comparison with*
869 *data*, *Phys. Rev. D* **96**(9), 096001 (2017), doi:[10.1103/PhysRevD.96.096001](https://doi.org/10.1103/PhysRevD.96.096001), [1708.](https://doi.org/10.1103/PhysRevD.96.096001)
870 [03303](https://doi.org/10.1103/PhysRevD.96.096001).

- 871 [93] R. J. Hill, P. Kammel, W. J. Marciano and A. Sirlin, *Nucleon Axial Radius and Muonic*
872 *Hydrogen — A New Analysis and Review*, Rept. Prog. Phys. **81**(9), 096301 (2018),
873 doi:[10.1088/1361-6633/aac190](https://doi.org/10.1088/1361-6633/aac190), [1708.08462](https://arxiv.org/abs/1708.08462).
- 874 [94] S. Galster, H. Klein, J. Moritz, K. H. Schmidt, D. Wegener and J. Bleckwenn, *Elastic*
875 *electron-deuteron scattering and the electric neutron form factor at four-momentum*
876 *transfers $5\text{fm}^{-2} < q^2 < 14\text{fm}^{-2}$* , Nucl. Phys. B **32**, 221 (1971), doi:[10.1016/0550-](https://doi.org/10.1016/0550-3213(71)90068-X)
877 [3213\(71\)90068-X](https://doi.org/10.1016/0550-3213(71)90068-X).
- 878 [95] J. J. Krauth, M. Diepold, B. Franke, A. Antognini, F. Kottmann and R. Pohl,
879 *Theory of the $n=2$ levels in muonic deuterium*, Annals Phys. **366**, 168 (2016),
880 doi:[10.1016/j.aop.2015.12.006](https://doi.org/10.1016/j.aop.2015.12.006), [1506.01298](https://arxiv.org/abs/1506.01298).
- 881 [96] B. Franke, J. J. Krauth, A. Antognini, M. Diepold, F. Kottmann and R. Pohl, *Theory*
882 *of the $n = 2$ levels in muonic helium-3 ions*, Eur. Phys. J. D **71**(12), 341 (2017),
883 doi:[10.1140/epjd/e2017-80296-1](https://doi.org/10.1140/epjd/e2017-80296-1), [1705.00352](https://arxiv.org/abs/1705.00352).
- 884 [97] M. Diepold, B. Franke, J. J. Krauth, A. Antognini, F. Kottmann and R. Pohl, *Theory of*
885 *the Lamb shift and Fine Structure in muonic ^4He ions and the muonic $^3\text{He} - ^4\text{He}$ Isotope*
886 *Shift*, Annals Phys. **396**, 220 (2018), doi:[10.1016/j.aop.2018.07.015](https://doi.org/10.1016/j.aop.2018.07.015), [1606.05231](https://arxiv.org/abs/1606.05231).
- 887 [98] P. A. Zyla *et al.*, *Review of Particle Physics*, PTEP **2020**(8), 083C01 (2020),
888 doi:[10.1093/ptep/ptaa104](https://doi.org/10.1093/ptep/ptaa104).
- 889 [99] D. R. Phillips, G. Rupak and M. J. Savage, *Improving the convergence of NN effective*
890 *field theory*, Phys. Lett. B **473**, 209 (2000), doi:[10.1016/S0370-2693\(99\)01496-3](https://doi.org/10.1016/S0370-2693(99)01496-3),
891 [nucl-th/9908054](https://arxiv.org/abs/nuc1-th/9908054).
- 892 [100] C. E. Carlson, M. Gorchtein and M. Vanderhaeghen, *Nuclear structure contribu-*
893 *tion to the Lamb shift in muonic deuterium*, Phys. Rev. A **89**(2), 022504 (2014),
894 doi:[10.1103/PhysRevA.89.022504](https://doi.org/10.1103/PhysRevA.89.022504), [1311.6512](https://arxiv.org/abs/1311.6512).
- 895 [101] C. E. Carlson, M. Gorchtein and M. Vanderhaeghen, *Two-photon exchange correc-*
896 *tion to $2S - 2P$ splitting in muonic ^3He ions*, Phys. Rev. A **95**(1), 012506 (2017),
897 doi:[10.1103/PhysRevA.95.012506](https://doi.org/10.1103/PhysRevA.95.012506), [1611.06192](https://arxiv.org/abs/1611.06192).
- 898 [102] K. Pachucki and A. Wienczek, *Nuclear structure effects in light muonic atoms*, Phys. Rev.
899 A **91**(4), 040503 (2015), doi:[10.1103/PhysRevA.91.040503](https://doi.org/10.1103/PhysRevA.91.040503), [1501.07451](https://arxiv.org/abs/1501.07451).
- 900 [103] R. B. Wiringa, V. G. J. Stoks and R. Schiavilla, *An Accurate nucleon-nucleon*
901 *potential with charge independence breaking*, Phys. Rev. C **51**, 38 (1995),
902 doi:[10.1103/PhysRevC.51.38](https://doi.org/10.1103/PhysRevC.51.38), [nucl-th/9408016](https://arxiv.org/abs/nuc1-th/9408016).
- 903 [104] C. Ji, N. Nevo Dinur, S. Bacca and N. Barnea, *Nuclear Polarization Cor-*
904 *rections to the $\mu^4\text{He}^+$ Lamb Shift*, Phys. Rev. Lett. **111**, 143402 (2013),
905 doi:[10.1103/PhysRevLett.111.143402](https://doi.org/10.1103/PhysRevLett.111.143402), [1307.6577](https://arxiv.org/abs/1307.6577).
- 906 [105] O. J. Hernandez, C. Ji, S. Bacca, N. Nevo Dinur and N. Barnea, *Improved esti-*
907 *mates of the nuclear structure corrections in μD* , Phys. Lett. B **736**, 344 (2014),
908 doi:[10.1016/j.physletb.2014.07.039](https://doi.org/10.1016/j.physletb.2014.07.039), [1406.5230](https://arxiv.org/abs/1406.5230).
- 909 [106] N. Nevo Dinur, C. Ji, S. Bacca and N. Barnea, *Nuclear structure correc-*
910 *tions to the Lamb shift in $\mu^3\text{He}^+$ and $\mu^3\text{H}$* , Phys. Lett. B **755**, 380 (2016),
911 doi:[10.1016/j.physletb.2016.02.023](https://doi.org/10.1016/j.physletb.2016.02.023), [1512.05773](https://arxiv.org/abs/1512.05773).

- 912 [107] C. Ji, S. Bacca, N. Barnea, O. J. Hernandez and N. Nevo-Dinur, *Abinitio calculation*
913 *of nuclear structure corrections in muonic atoms*, J. Phys. G **45**(9), 093002 (2018),
914 doi:[10.1088/1361-6471/aad3eb](https://doi.org/10.1088/1361-6471/aad3eb), [1806.03101](https://arxiv.org/abs/1806.03101).
- 915 [108] S. Pastore, F. Myhrer and K. Kubodera, *An update of muon capture on hydrogen*, Int.
916 J. Mod. Phys. E **23**(08), 1430010 (2014), doi:[10.1142/S0218301314300100](https://doi.org/10.1142/S0218301314300100), [1405.1358](https://arxiv.org/abs/1405.1358).
917
- 918 [109] B. Lauss and B. Blau, *UCN, the ultracold neutron source – neutrons for particle physics*,
919 SciPost Phys. Proc. **2**, ppp (2021), doi:[10.21468/SciPostPhysProc.2.XXX](https://doi.org/10.21468/SciPostPhysProc.2.XXX).
- 920 [110] B. Fornal and B. Grinstein, *Dark Matter Interpretation of the Neutron Decay Anomaly*,
921 Phys. Rev. Lett. **120**(19), 191801 (2018), doi:[10.1103/PhysRevLett.120.191801](https://doi.org/10.1103/PhysRevLett.120.191801), [Er-
922 ratum: Phys.Rev.Lett. 124, 219901 (2020)], [1801.01124](https://arxiv.org/abs/1801.01124).
- 923 [111] A. Czarnecki, W. J. Marciano and A. Sirlin, *Neutron Lifetime and Axial Coupling Connec-*
924 *tion*, Phys. Rev. Lett. **120**(20), 202002 (2018), doi:[10.1103/PhysRevLett.120.202002](https://doi.org/10.1103/PhysRevLett.120.202002),
925 [1802.01804](https://arxiv.org/abs/1802.01804).
- 926 [112] T. D. Lee and C.-N. Yang, *Question of Parity Conservation in Weak Interactions*, Phys.
927 Rev. **104**, 254 (1956), doi:[10.1103/PhysRev.104.254](https://doi.org/10.1103/PhysRev.104.254).
- 928 [113] N. Severijns, M. Beck and O. Naviliat-Cuncic, *Tests of the standard electroweak model*
929 *in beta decay*, Rev. Mod. Phys. **78**, 991 (2006), doi:[10.1103/RevModPhys.78.991](https://doi.org/10.1103/RevModPhys.78.991),
930 [nucl-ex/0605029](https://arxiv.org/abs/nucl-ex/0605029).
- 931 [114] F. Hagelstein, R. Miskimen and V. Pascalutsa, *Nucleon Polarizabilities: from*
932 *Compton Scattering to Hydrogen Atom*, Prog. Part. Nucl. Phys. **88**, 29 (2016),
933 doi:[10.1016/j.ppnp.2015.12.001](https://doi.org/10.1016/j.ppnp.2015.12.001), [1512.03765](https://arxiv.org/abs/1512.03765).
- 934 [115] B. Ananthanarayan, G. Colangelo, J. Gasser and H. Leutwyler, *Roy equation analysis of*
935 *$\pi\pi$ scattering*, Phys. Rept. **353**, 207 (2001), doi:[10.1016/S0370-1573\(01\)00009-6](https://doi.org/10.1016/S0370-1573(01)00009-6),
936 [hep-ph/0005297](https://arxiv.org/abs/hep-ph/0005297).
- 937 [116] I. Caprini, G. Colangelo and H. Leutwyler, *Regge analysis of the $\pi\pi$ scattering amplitude*,
938 Eur. Phys. J. C **72**, 1860 (2012), doi:[10.1140/epjc/s10052-012-1860-1](https://doi.org/10.1140/epjc/s10052-012-1860-1), [1111.7160](https://arxiv.org/abs/1111.7160).
- 939 [117] R. Garcia-Martin, R. Kaminski, J. R. Pelaez, J. Ruiz de Elvira and F. J. Yndurain, *The Pion-*
940 *pion scattering amplitude. IV: Improved analysis with once subtracted Roy-like equations*
941 *up to 1100 MeV*, Phys. Rev. D **83**, 074004 (2011), doi:[10.1103/PhysRevD.83.074004](https://doi.org/10.1103/PhysRevD.83.074004),
942 [1102.2183](https://arxiv.org/abs/1102.2183).
- 943 [118] J. Gasser, V. E. Lyubovitskij and A. Rusetsky, *Hadronic atoms in QCD + QED*, Phys. Rept.
944 **456**, 167 (2008), doi:[10.1016/j.physrep.2007.09.006](https://doi.org/10.1016/j.physrep.2007.09.006), [0711.3522](https://arxiv.org/abs/0711.3522).
- 945 [119] M. Hoferichter, J. Ruiz de Elvira, B. Kubis and U.-G. Meißner, *Roy–Steiner-*
946 *equation analysis of pion–nucleon scattering*, Phys. Rept. **625**, 1 (2016),
947 doi:[10.1016/j.physrep.2016.02.002](https://doi.org/10.1016/j.physrep.2016.02.002), [1510.06039](https://arxiv.org/abs/1510.06039).
- 948 [120] T. Das, G. S. Guralnik, V. S. Mathur, F. E. Low and J. E. Young, *Electromagnetic mass*
949 *difference of pions*, Phys. Rev. Lett. **18**, 759 (1967), doi:[10.1103/PhysRevLett.18.759](https://doi.org/10.1103/PhysRevLett.18.759).
- 950 [121] J. F. Donoghue and A. F. Perez, *The Electromagnetic mass differences of pions and kaons*,
951 Phys. Rev. D **55**, 7075 (1997), doi:[10.1103/PhysRevD.55.7075](https://doi.org/10.1103/PhysRevD.55.7075), [hep-ph/9611331](https://arxiv.org/abs/hep-ph/9611331).

- 952 [122] B. Ananthanarayan and B. Moussallam, *Electromagnetic corrections in the anomaly sec-*
953 *tor*, JHEP **05**, 052 (2002), doi:[10.1088/1126-6708/2002/05/052](https://doi.org/10.1088/1126-6708/2002/05/052), [hep-ph/0205232](https://arxiv.org/abs/hep-ph/0205232).
- 954 [123] K. Kampf and B. Moussallam, *Chiral expansions of the π^0 lifetime*, Phys. Rev. D **79**,
955 076005 (2009), doi:[10.1103/PhysRevD.79.076005](https://doi.org/10.1103/PhysRevD.79.076005), [0901.4688](https://arxiv.org/abs/0901.4688).
- 956 [124] P. Masjuan and P. Sanchez-Puertas, *Pseudoscalar-pole contribution to the $(g_\mu - 2)$: a ratio-*
957 *nal approach*, Phys. Rev. D **95**(5), 054026 (2017), doi:[10.1103/PhysRevD.95.054026](https://doi.org/10.1103/PhysRevD.95.054026),
958 [1701.05829](https://arxiv.org/abs/1701.05829).
- 959 [125] M. Hoferichter, B.-L. Hoid, B. Kubis, S. Leupold and S. P. Schneider, *Dispersion*
960 *relation for hadronic light-by-light scattering: pion pole*, JHEP **10**, 141 (2018),
961 doi:[10.1007/JHEP10\(2018\)141](https://doi.org/10.1007/JHEP10(2018)141), [1808.04823](https://arxiv.org/abs/1808.04823).
- 962 [126] A. Gérardin, H. B. Meyer and A. Nyffeler, *Lattice calculation of the pion transition*
963 *form factor with $N_f = 2 + 1$ Wilson quarks*, Phys. Rev. D **100**(3), 034520 (2019),
964 doi:[10.1103/PhysRevD.100.034520](https://doi.org/10.1103/PhysRevD.100.034520), [1903.09471](https://arxiv.org/abs/1903.09471).
- 965 [127] D. A. Bryman, P. Depommier and C. Leroy, *$PI \rightarrow E$ neutrino, $PI \rightarrow E$ neutrino*
966 *gamma decays and related processes*, Phys. Rept. **88**, 151 (1982), doi:[10.1016/0370-](https://doi.org/10.1016/0370-1573(82)90162-4)
967 [1573\(82\)90162-4](https://doi.org/10.1016/0370-1573(82)90162-4).
- 968 [128] V. Cirigliano, M. Knecht, H. Neufeld and H. Pichl, *The Pionic beta decay in chiral per-*
969 *turbation theory*, Eur. Phys. J. C **27**, 255 (2003), doi:[10.1140/epjc/s2002-01093-2](https://doi.org/10.1140/epjc/s2002-01093-2),
970 [hep-ph/0209226](https://arxiv.org/abs/hep-ph/0209226).
- 971 [129] V. Cirigliano, S. Gardner and B. Holstein, *Beta Decays and Non-Standard Interactions in*
972 *the LHC Era*, Prog. Part. Nucl. Phys. **71**, 93 (2013), doi:[10.1016/j.ppnp.2013.03.005](https://doi.org/10.1016/j.ppnp.2013.03.005),
973 [1303.6953](https://arxiv.org/abs/1303.6953).